

**Effect of a novel framework design in ceria-stabilized
zirconia/alumina nanocomposite (Ce-TZP/A)-based
all-ceramic crowns**

**Inaugural-Dissertation
zur Erlangung des Doktorgrades
der Zahnheilkunde**

**der Medizinischen Fakultät
der Eberhard Karls Universität
zu Tübingen**

vorgelegt von

Sawada, Tomofumi

2016

Dekan: Professor Dr. I.B.Autenrieth

1.Berichterstatter: Professor Dr. J.Geis-Gerstorfer

2.Berichterstatter: Professor Dr. H.Weber

To my beloved parents and wife for their constant support and understanding

Content	4
List of Tables	7
List of Figures	8
List of Abbreviations	11
1.0 Introduction	12
1.1 All-ceramic dental restorations	12
1.2 Computer-Aided Design/Computer-Aided Manufacturing (CAD/CAM)	14
1.3 Zirconia	15
1.4 Ceria-stabilized zirconia/alumina nanocomposite (Ce-TZP/A)	18
1.5 Clinical performance of bilayered porcelain/zirconia ceramics	19
1.6 Complication of bilayered porcelain/zirconia ceramics	22
1.7 Framework modification of zirconia	23
1.8 Aim of this study	25
2.0 Material and methods	27
2.1 Fabrication of zirconia framework	27
2.1.1 Tooth preparation	27
2.1.2 Manufacturing of metal tooth analogs	29
2.1.3 CAD/CAM process	31
2.1.4 Fabrication of Ce-TZP/A frameworks	33
2.2 Veneering porcelain on Ce-TZP/A frameworks	36
2.2.1 Pretreatment of framework surfaces	36
2.2.2 Layering process	37

2.3	Cementation of Ce-TZP/A crowns	41
2.3.1	Manufacturing of resin tooth analogs	42
2.3.2	Pretreatment of abutment tooth analog surfaces	42
2.3.3	Pretreatment of crown inner surfaces	43
2.3.4	Cementation of Ce-TZP/A-based crowns	43
2.4	Fixation	44
2.4.1	Manufacturing of acrylic disk blocks	44
2.4.2	Fixation of the specimens to acrylic disk blocks	44
2.5	Mechanical preloading by chewing simulation	44
2.6	Fracture loading test	46
2.7	Analysis of failure mode	47
2.8	Statistical analysis	49
3.0	Results	50
3.1	Chewing simulation	50
3.2	Fracture load	51
3.3	Failure mode	54
3.3.1	Failure mode description	54
3.3.2	Failure mode ratio	65
4.0	Discussion	66
4.1	Framework design	66
4.2	Fracture load	68
4.3	Failure mode	72

5.0 Conclusions	75
6.0 Summary	76
7.0 Zusammenfassung	77
8.0 Author contribution	79
9.0 References	80
10.0 Appendix	88
10.1 Microscopy and SEM of prefailure in Ce-TZP/A crown after mechanical preloading	88
10.2 Details of distribution of failure modes in Ce-TZP/A crowns with different framework designs	89
10.3 Analysis of fracture loads in different failure modes	90
11.0 Acknowledgments	92
12.0 Curriculum Vitae	93

List of Tables

Table 1. Characteristics of ceria-stabilized zirconia/alumina nanocomposite (Ce-TZP/A).

Table 2. Clinical performance of zirconia-based all-ceramic restorations in systematic reviews.

Table 3. Complications of bilayered porcelain/zirconia ceramics.

Table 4. Materials used in the study.

Table 5. Experimental groups.

Table 6. Time schedule of porcelain firing.

Table 7. Classification of failure modes.

Table 8. Fracture loads of all-ceramic crowns using different Ce-TZP/A frameworks.

Table 9. Number of failure modes of all-ceramic crowns using different Ce-TZP/A frameworks.

Table 10. Distribution of failure modes in Ce-TZP/A crowns with different framework designs.

List of Figures

Figure 1. Classification of all-ceramic materials.

Figure 2. Factors that may help prevent complications in zirconia-based all-ceramic restorations.

Figure 3. Study outline.

Figure 4. Melamine formaldehyde resin tooth model.

Figure 5. Abutment tooth preparation for all-ceramic crown.

Figure 6. Wax-up of the prepared abutment tooth.

Figure 7. Casting machine.

Figure 8. Co-Cr tooth analog.

Figure 9. Ce-TZP/A blanks.

Figure 10. Digital scanner.

Figure 11. Framework design by a CAD software.

Figure 12. Ce-TZP/A frameworks.

Figure 13. Supporting structures.

Figure 14. Dental porcelain furnace.

Figure 15. Ce-TZP/A framework after wash-bake firing.

Figure 16. Process of veneering porcelain.

Figure 17. Ce-TZP/A-based all-ceramic crown after glazing firing.

Figure 18. Resin tooth analog.

Figure 19. Original loading device for cementation of Ce-TZP/A-based crowns.

Figure 20. Fixation of a specimen to an acrylic disk block.

Figure 21. Masticator.

Figure 22. Antagonist and three-point contact with the fixed specimen.

Figure 23. Universal testing machine.

Figure 24. Fracture loading test.

Figure 25. Stereomicroscopy.

Figure 26. Scanning electron microscopy.

Figure 27. Failure mode classification.

Figure 28. Photographs of prefailure after mechanical preloading in Group 1(+).

Figure 29. Fracture loads in experimental groups without mechanical preloading.

Figure 30. Fracture loads in experimental groups with mechanical preloading.

Figure 31. Comparison of fracture load results regarding the chewing simulation in each experimental group.

Figure 32. Stereomicroscopy of Ce-TZP/A crowns in Groups 1–4(-).

Figure 33. Stereomicroscopy of Ce-TZP/A crowns in Groups 1–4(+).

Figure 34. Scanning electron microscopy of Ce-TZP/A crown from Group 1(-).

Figure 35. Scanning electron microscopy of Ce-TZP/A crown from Group 2(-).

Figure 36. Scanning electron microscopy of Ce-TZP/A crown from Group 3(-).

Figure 37. Scanning electron microscopy of Ce-TZP/A crown from Group 4(-).

Figure 38. Scanning electron microscopy of Ce-TZP/A crown from Group 1(+).

Figure 39. Scanning electron microscopy of Ce-TZP/A crown from Group 2(+).

Figure 40. Scanning electron microscopy of Ce-TZP/A crown from Group 3(+).

Figure 41. Scanning electron microscopy of Ce-TZP/A crown from Group 4(+).

Figure 42. Stereomicroscopy and scanning electron microscopy observations of porcelain chipping.

Figure 43. Scanning electron microscopy comparison of failure progression.

Figure 44. Stereomicroscopy observation of chipping of porcelain veneer

(buccal side aspect) in Group 4.

Figure 45. Failure mode ratios.

Figure 46. Stereomicroscopy and scanning electron microscopy of Ce-TZP/A crown from Group 1(+) with prefailure after mechanical preloading.

Figure 47. Fracture load in each failure mode.

Figure 48. Comparison of fracture loads between different failure modes.

List of Abbreviations

ANOVA: Analysis of variance

Al_2O_3 : Aluminum oxide, Alumina

CAD/CAM: Computer-Aided Design/Computer-Aided Manufacturing

CaO: Calcium oxide

CeO_2 : Cerium oxide

Ce-TZP/A: Ceria-stabilized zirconia/alumina nanocomposite

Co-Cr: Cobalt-Chrome

CTE: Coefficient of thermal expansion

FPD: Fixed partial denture

MgO: Magnesium oxide

MPa: Megapascal

LTAD: Low-temperature aging degradation

SEM: Scanning electron microscope

TiO_2 : Titanium oxide

TZP: Tetragonal zirconia polycrystalline

Y-TZP: Yttrium partially stabilized tetragonal zirconia polycrystalline

Y_2O_3 : Yttrium oxide

ZrO_2 : Zirconia

1.0 Introduction

1.1 All-ceramic dental restorations

All-ceramic dental restorations, a restorative/prosthetic treatment to reconstruct defective or missing teeth, include partial veneer crowns (i.e., inlays, onlays, and laminate veneers), full veneer crowns, and fixed partial dentures (FPDs).

The use of all-ceramic restorations began more than 100 years ago (Gracis et al. 2015), and porcelain has often been used in dental ceramics (Miyazaki et al. 2013). Although adaptations of dental ceramics have been limited by the brittleness of porcelain, conventional esthetic treatments have used this material fused to metal restorations. Dental ceramics have since been developed and improved, with current types of all-ceramic restorations divided broadly into two categories according to the materials used (Larsson and Wennerberg 2014; Gracis et al. 2015) (Figure 1). These newer materials have made it possible to reproduce an optical transparency similar to that of natural teeth, offering highly esthetic prostheses (Donovan 2008). Because all-ceramic restorations have good biocompatibility and help satisfy patient demands of esthetics, their use has superseded that of porcelain-fused-metal ceramic restorations (Miyazaki et al. 2013). Metal-free materials are desirable for patient health; however, hypoallergenic nonmetal materials such as resin and fiber-reinforced resin are insufficient for use in posterior regions in esthetic dentistry because of their mechanical properties and tendency to become discolored (Kolbeck et al. 2006; Omata et al. 2006; Tuncdemir and Aykent 2012).

For successful treatment in clinical practice, a dentist would select ceramic materials after a consultation with the patient and dental technicians, with consideration of regions and sizes. Predominantly glassy ceramics are highly esthetic, whereas polycrystalline ceramics are much less esthetic and are meant to be used solely as framework material (Gracis et al. 2015). All-ceramic restoration systems comprise two main types (Miyazaki et al. 2013): (1) full-contour crowns used as a single material, and (2) bilayered ceramics, which are esthetic ceramics fused to frameworks.

In the former system, feldspathic porcelain was originally used in a conventional build-up technique; more recently, reinforced glassy ceramics such as lithium disilicate have been successfully used to make single crowns by casting or the press technique. Consequently, the use of nonoxide-based ceramic restorations, such as porcelain and glass-ceramics, has been limited to small anterior restorations because of the risk of complete fracture (Larsson and Wennerberg 2014).

In the latter system, frameworks (copings) were made from oxide-based ceramics such as zirconia, and feldspathic porcelain was veneered onto the framework to make single crowns or FPDs for use in molar regions. Although oxide-based ceramics have superior mechanical properties compared with nonoxide-based ceramics, they are difficult to process. To remedy this, a novel system, computer-aided design/computer-aided manufacturing (CAD/CAM) was developed in the 1970s (Mörmann et al. 1989; Duret and Preston 1991; Andersson and Odén 1993).

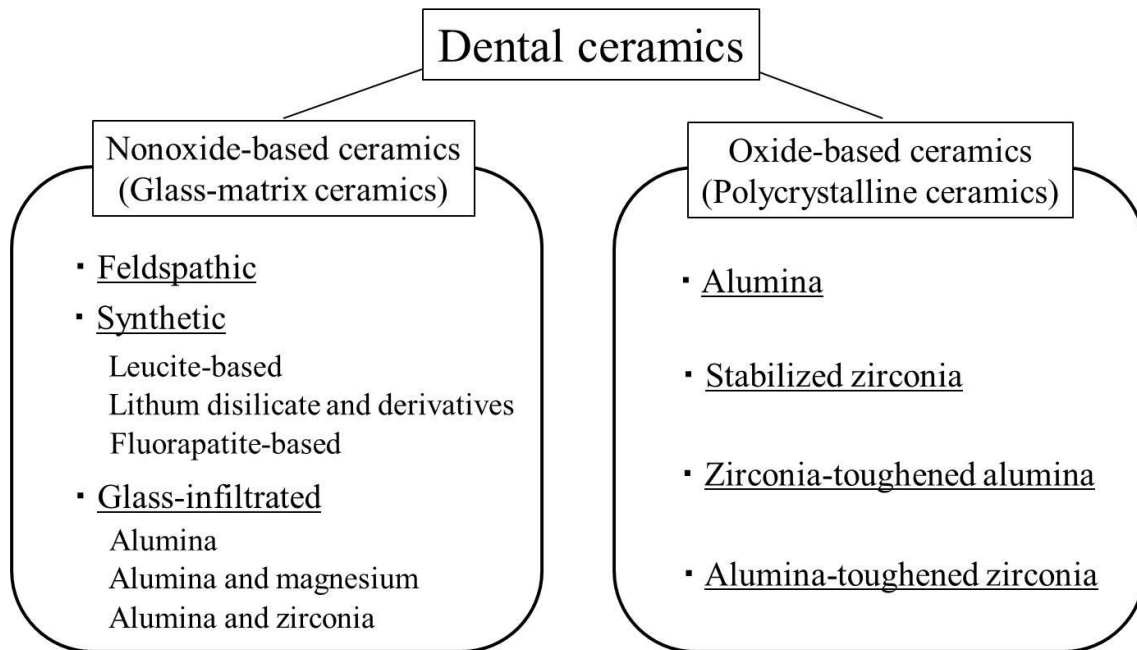


Figure 1. Classification of all-ceramic materials (Larsson and Wennerberg 2014; Gracis et al. 2015).

1.2 Computer-Aided Design/Computer-Aided Manufacturing (CAD/CAM)

The use of all-ceramic prostheses in restorative treatments has become popular, and many of these restorations can be fabricated using either traditional laboratory methods or CAD/CAM machining (Li et al. 2014). CAD/CAM is a novel system for dental laboratory work that has shifted the manufacturing process partially or fully from handwork to computer-controlled work, saving time and suppressing variations in quality. CAM/CAM techniques have been used in dentistry for over 30 years, and can now be used to fabricate dental restorative and prosthetic devices (Miyazaki et al. 2009; Rekow 1991).

An overview of the CAD/CAM system is as follows: first, after tooth preparation, either an impression of the abutment tooth is taken and used to make a stone model that is then scanned, or an optical impression is obtained directly using an intraoral scanner. Digitized data are then reconstructed as three-dimensional (3-D) graphics, and the morphology of restorative/prosthetic devices is virtually designed on the monitor. Finally, restorative/prosthetic devices are fabricated by milling a ceramic block or blank using a numerically-controlled machine (Miyazaki et al. 2013).

In the early days of dental CAD/CAM use, prosthesis quality suffered from low fitting accuracy (Boitelle et al. 2014), which induced problems with microleakage (Rossetti et al. 2008), adaptation, retention (Thompson and Rekow 2004), and secondary caries (Sailer et al. 2006). However, quality was improved by the development of scanning and milling abilities of the CAD/CAM system. A recent systematic review concluded that the fit accuracy of milled CAD/CAM restorations is improved compared with that obtained using conventional press or casting techniques (Boitelle et al. 2014). The use of zirconia for all-ceramic restorations using the CAD/CAM system has thereby increased (Denry and Kelly 2008).

1.3 Zirconia

Before its application in the dental field, the ceramic biomaterial zirconia (ZrO_2), had been in use in the field of medicine since 1985 (Clarke et al. 2003). In orthopedics, zirconia balls made from yttrium partially stabilized tetragonal zirconia polycrystalline (Y-TZP) had been used as biomedical implants of femoral heads in total hip

arthroplasty (Christel et al. 1988). The flexural strength of zirconia (> 1500 MPa) was two to three times higher than that of alumina (500–580 MPa) (Cales 2000; Blaise et al. 2001). Briefly, zirconia was one of the strongest ceramics suitable for medical use (Clarke et al. 2003).

Zirconia has been widely used in all-ceramic dental restorations over the past decade (Miyazaki and Hotta 2011). Pure zirconia can exist in three allotropic forms (phases), termed monoclinic (room temperature), tetragonal (1170° C), and cubic (2370° C) (Clarke et al. 2003). The addition of oxides such as yttrium oxide (Y_2O_3), calcium oxide (CaO), and magnesium oxide (MgO) to zirconia stabilizes the tetragonal phase at room temperature. Dental zirconia consists mainly of the tetragonal phase stabilized with 3 mol% Y_2O_3 (Y-TZP), which has high fracture toughness and flexural strength (Miyazaki et al. 2013; Gracis et al. 2015) and is commonly used in the framework of dental prostheses. In particular, Y-TZP enabled the application of long-span FPD in the molar regions (Roediger et al. 2010; Schley et al. 2010). Because of the superior mechanical properties of Y-TZP, framework fractures were rare incidences in this material compared with other ceramics (Guazzato et al. 2004; Vult von Steyern et al. 2006). Zirconia is presently the only ceramic material that has strength similar to that of metal.

When a crack is initiated on the surface of Y-TZP, the concentration of force at the top of the crack causes tetragonal-to-monoclinic phase transformation accompanied by shear strain and a 4% increase in volume (Clarke et al. 2003; Miyazaki et al. 2013). In the vicinity of a propagating crack, this stress-induced transformation causes

compressive stress that shields the crack tip from the applied stress and enhances fracture toughness (Hannink et al. 2000).

However, this transformation from the tetragonal to the monoclinic phase may have catastrophic results under certain hydrothermal conditions, a tendency that increases with aging (Chevalier 2006). In other words, one risk of Y-TZP is its susceptibility to structural transformation by low-temperature aging degradation (LTAD). The degradation of Y-TZP is caused by the micro- and macrocracking that accompanies this transformation, which proceeds rapidly at temperatures of 200-300° C (Yoshimura et al. 1987; Tanaka et al. 2003). Moreover, this degradation is time-dependent and enhanced by water or water vapor. LTAD is also considered to result from long-term Y-TZP use in the dental field (Cattani-Lorente et al. 2011).

Conversely, some researchers had reported the opposing findings. No serious decrease of bending strength was found after time-dependent changes in zirconia placed in saline solution at 95° C for over 3 years (Shimizu et al. 1993). Further, thermal cycling and mechanical loading showed no negative effects such as phase transformation on the biaxial strength of Y-TZP (Bankoğlu Güngör et al. 2014).

Thus, the influence of LTAD on Y-TZP frameworks in long-term clinical use is still unclear. In consideration of this undesirable characteristic of Y-TZP, Nawa et al. (1998) developed ceria-stabilized zirconia/alumina nanocomposite (Ce-TZP/A) as a novel zirconia ceramic.

1.4 Ceria-stabilized zirconia/alumina nanocomposite (Ce-TZP/A)

Ce-TZP has much higher fracture toughness but lower flexural strength and hardness than Y-TZP (Tsukuma and Shimada 1985), and has therefore never been applied in the dental field (Miyazaki et al. 2013). Ce-TZP/A was developed by combining zirconia and alumina using nanotechnology to improve strength, and exhibits fracture strength superior to that of Y-TZP (Omori et al. 2013).

Ce-TZP/A is composed of 70 vol% TZP stabilized with 10 mol% CeO₂ (ceria), 30 vol% Al₂O₃, and 0.05 mol% TiO₂ (Tanaka et al. 2003). This material has an interpenetrated intragranular nanostructure, in which nanometer-sized particles of Ce-TZP and Al₂O₃ localize within submicron-sized grains of Al₂O₃ and Ce-TZP, respectively (Ban et al. 2008).

One advantage of Ce-TZP/A is that it is not influenced by LTAD. After autoclaving, Y-TZP showed remarkable increases in monoclinic zirconia content (0.3 vol% before, 49.9 vol% after) and a slight decrease in biaxial flexure strength (1046 MPa before, 892 MPa after), whereas Ce-TZP/A showed no significant difference in monoclinic content (4.8–5.5 vol%) or biaxial flexure strength (1371–1422 MPa) after storage under any examined conditions (Ban et al. 2008). Moreover, in an *in vitro* study, the smooth surface of Ce-TZP/A showed less wear compared with that of Y-TZP, indicating that it is durable and suffers fewer harmful effects for antagonist such as human enamel and ceramic materials (Aldegheishem et al. 2015).

The superior characteristics of Ce-TZP/A give it potential as a novel framework and suggest that it may resist chipping during long-term use in all-ceramic restorations (Table 1). Unfortunately, there have been only 2 reports of short-term clinical use of Ce-TZP/A frameworks (Philipp et al. 2010; Tanaka et al. 2015), and evidence regarding its long-term clinical use and the influence of framework design is scarce.

Table 1. Characteristics of ceria-stabilized zirconia/alumina nanocomposite (Ce-TZP/A).

	Unit	Properties
Material		Ce-TZP/A
Composition		ZrO ₂ , Al ₂ O ₃ , CeO ₂ , TiO ₂
Density	g/cm ³	5.5
Flexural strength	MPa	1400
Fracture toughness	MPa m ^{1/2}	17
Coefficient of thermal expansion (CTE)	10 ⁻⁶ K ⁻¹	10.0±0.5
Vickers Hardness	GPa	11.5
Elastic modulus	GPa	240
Thermal conductivity	W/mK	6.2
Total light transmittance		≅0% (t=1.0 mm)
Radioactivity	Bq/g	0.67
Solubility	µg/cm ²	0

1.5 Clinical performance of bilayered porcelain/zirconia ceramics

Conventional reliable ceramic restoration has used metal-ceramic restorations, which have showed high survival rates over the past two decades. For esthetic and biocompatibility reasons, alternative all-ceramic restorations have been applied; however, the survival rate of all-ceramic restorations was lower than or similar to that

of metal-ceramics. In a previous study, estimated 5-year survival rates for all-ceramic crowns and metal-ceramic crowns were 93.3% and 95.6%, respectively (Pjetursson et al. 2007). Wittneben et al. (2009) also reported that before application of zirconia, the estimated 5-year survival rate of all-ceramic restorations using glass-matrix ceramics for partial veneer crowns in the posterior region was 91.6%. However, these materials had a lower survival rate in the posterior region. Glass-ceramic and InCeram in particular had low survival rates of 84.4% and 90.4%, respectively (Pjetursson et al. 2007). Glass-matrix ceramics were thus determined to be suitable for clinical use as inlays, onlays, crowns, and three-unit FPDs in the anterior region (Gracis et al. 2015).

After improvement of the CAD/CAM system and ceramic materials, the success rate of zirconia-based all-ceramics is adequate-comparable to that of conventional porcelain-fused-to-metal crowns (Heintze and Rousson 2010; Pelaez et al. 2012). The cumulative 5-year survival rate of bilayered porcelain/zirconia ceramics for crowns was found to be 95.9% (Larsson and Wennerberg 2014), and the survival rate of zirconia was similar to that of leucite or lithium-disilicate reinforced glass ceramic (96.6%), glass-infiltrated alumina (94.6%), and densely sintered alumina (96%) in single crowns (Sailer et al. 2015). The estimated 5-year survival rate of bilayered porcelain/zirconia ceramics for FPDs was 94.29 % (Schley et al. 2010) from 1999 to 2009 (Table 2). In a recent systematic review, the survival rate of zirconia-based FPDs (90.4%) was higher than that of reinforced glass ceramic FPDs (89.1%) and glass-infiltrated alumina FPDs (86.2%) (Pjetursson et al. 2015).

Table 2. Clinical performance of zirconia-based all-ceramic restorations in systematic reviews.

Authors	Articles	Region	Prostheses	Number	Survival rate (%)	Complication rate (%)	Failures	Complications
Pjetursson et al. (2007)	34	Anterior	Cr	6006 (1765)	93.3	Technical: 2.8	-	-
		Posterior			(estimated)	Biological: 2.1		
		(Metal)			(95.6)	(Technical: 0.7) (Biological: 2.1)		
Schley et al. (2010)	18	Posterior	FPDs	330 (310: 3 or 4 units) (20: > 4 units)	94.3 (estimated)	Technical: 23.59 Biological: 8.18 (estimated)	19	Technical: 51 Biological: 29
Larsson and Wennerberg (2014)	12 (tooth-supported)	-	Cr	568	95.9	5.6	Technical: 16	Technical: 30
	16 (total)				(cumulative)	(cumulative)	Biological: 15	Biological: 27

Cr; crown, FPDs; fixed partial dentures. The parentheses around the numbers showed the metal-ceramic restorations for comparison.

1.6 Complications of bilayered porcelain/zirconia ceramics

Evaluation of the clinical performance of bilayered porcelain/zirconia ceramics has been complicated because of differences in criteria, number of cases, surface treatments (Pereira et al. 2015), veneering procedures, cementations (Karimipour-Saryazdi et al. 2010; Miragaya et al. 2011), framework designs (Okabayashi et al. 2013), and CAD/CAM systems. However, various complications of all-ceramic prostheses under any condition may be encountered during the regular dental checkup (Table 3).

Table 3. Complications of bilayered porcelain/zirconia ceramics.

(1) Technical complication	<ul style="list-style-type: none">•Cracking (or minor chipping) of veneering materials•Chipping of veneering materials•Framework fractures•Loss of retention•Marginal discrepancy
(2) Biological complication	<ul style="list-style-type: none">•Secondary caries•Endodontic problems•Tooth fractures•Periodontal diseases

For zirconia-based all-ceramic crowns, in a 2014 study by Larsson and Wennerberg, technical and biological reasons for failure are equally common. The most common complications have been identified as loss of retention, endodontic treatment, veneering material fractures, and bleeding on probing. The most common technical failures in glass-matrix ceramics are fractures of the restorations or of the tooth (Wittneben et al. 2009). In these cases, the present prostheses normally have to be removed and replaced by a new prostheses. No fracture of zirconia has been observed,

similar to metal FDP frameworks (Pelaez et al. 2012), as zirconia has superior mechanical properties; however, technical complications such as chipping of porcelain veneer of bilayered porcelain/zirconia ceramics have been noted (Larsson and Wennerberg 2014). Zirconia-based all-ceramic restorations have a high rate of fracture, ranging from 6% to 15% over a 3- to 5-year period, while the fracture rate for metal-ceramic restorations ranges from 4% to 10% over 10 years (Agustín-Panadero et al. 2014). In particular, the frequency of chipping of veneering porcelain is higher in zirconia FPDs than in porcelain-fused-to-metal ceramic FPDs (Heintze and Rousson 2010).

1.7 Framework modification of zirconia

Various factors may help prevent complications and allow successful use of zirconia-based all-ceramic restorations (Figure 2). Framework modification is one of the most important factors for reducing technical complications. The conventional uniform-thickness design of zirconia frameworks has been modified to create support cusps, yielding a more anatomical shape and an even thickness in the veneering porcelain (Rosentritt et al. 2009; Ferrari et al. 2014). These changes have been found to increase fracture strength and fatigue reliability, and thus reduce the chipping area of Y-TZP crowns (Kokubo et al. 2011; Guess et al. 2013). Unfortunately, they are insufficient to completely eliminate chipping in clinical practice (Beuer et al. 2010), because there are areas of porcelain that are unsupported by the zirconia framework.

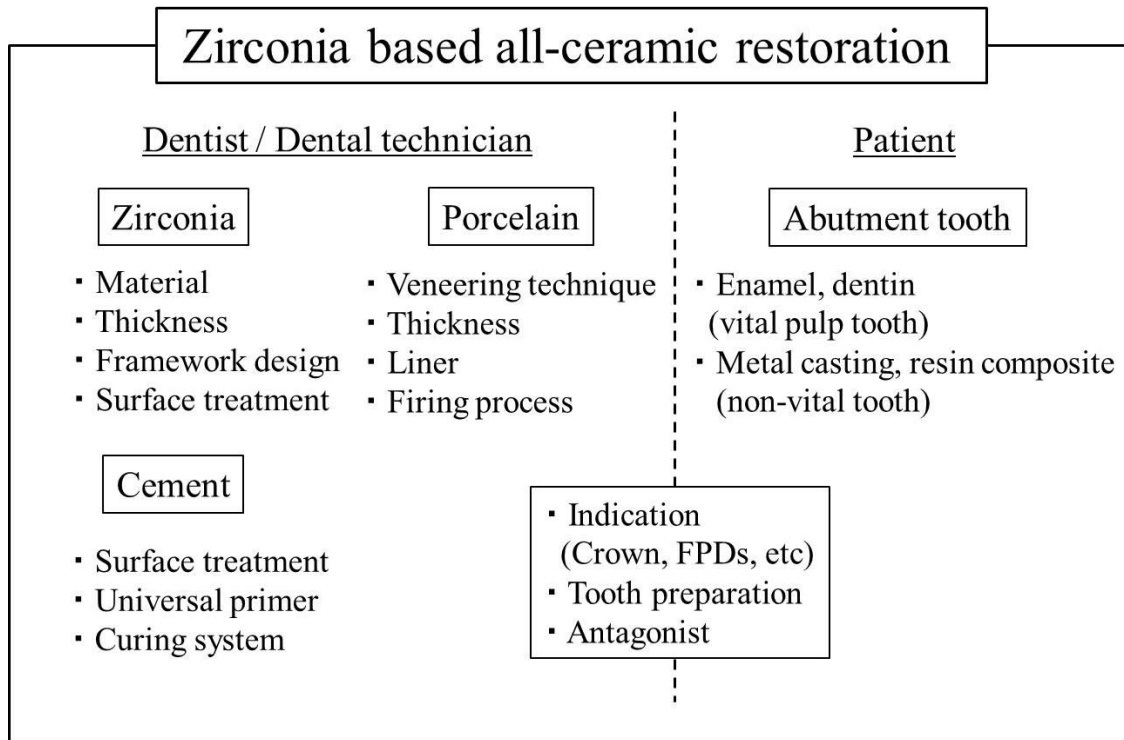


Figure 2. Factors that may help prevent complications in zirconia-based all-ceramic restorations. FPDs; fixed partial dentures.

Therefore, the anatomical shape has been further modified by extending the height by 2.0 mm in the lingual cervical margin and the thickness by 1.0 mm in the proximal area (lingual supporting structure); this shape has been clinically tested (Marchack et al. 2008) and exhibits higher fracture strength than previous anatomical shapes (Bonfante et al. 2010). However, the lingual supporting structure—though it adds resistance to occlusal force—has not been shown to improve the fatigue resistance of Y-TZP (Lorenzoni et al. 2010); an additional supporting structure has been shown necessary to prevent chipping in the unsupported buccal cusp (Silva et al. 2011).

Other researchers have proposed different framework modification; (1) the shoulder collar variations were incremental increases of 1-3mm in proximal and lingual height,

and/or buccal height respectively (Ha et al. 2013), (2) the additional parts of core material were made on the buccal and lingual sides (Tinscherrt et al. 2008), and (3) the support of veneering porcelain at the cusp tips and around the axial surfaces were designed (Broseghini et al. 2014).

1.8 Aim of this study

The aim of this study was to evaluate the fracture properties of all-ceramic crowns using different framework designs of ceria-stabilized zirconia/alumina nanocomposite (Ce-TZP/A).

The null hypotheses were that Ce-TZP/A-based all-ceramic crowns using a framework design with additional buccal and/or lingual supporting structures would not improve (1) fracture load or (2) failure mode. The study outline is given below (Figure 3).

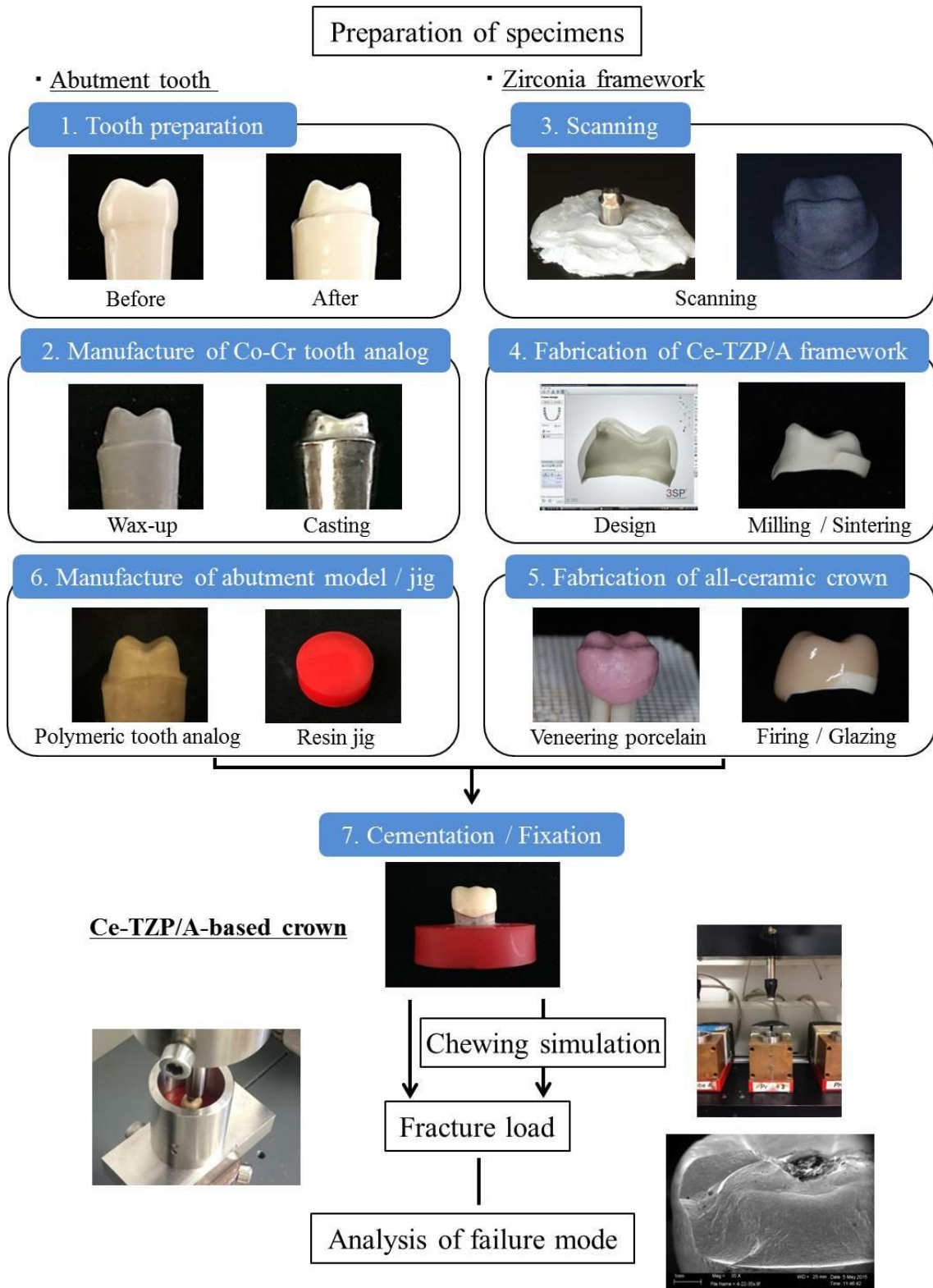


Figure 3. Study outline.

2.0 Materials and methods

2.1 Fabrication of zirconia framework

Four different zirconia frameworks made of Ce-TZP/A were fabricated by dental CAD/CAM, in which a metal tooth analog was scanned as a replica of the prepared abutment tooth, and frameworks were designed and milled out ($n = 96$). Materials used in this study are given in Table 4.

2.1.1 Tooth preparation

An artificial left mandibular first molar tooth (Simple Root Tooth Model A50-A-500, Nissin Dental Products Inc., Kyoto, Japan) made of melamine formaldehyde resin was used as an abutment tooth model (Figure 4, Figure 5 a, b). Abutment tooth preparation for all-ceramic crown was performed on the artificial tooth in the standard manner, i.e., with a 2.0-mm occlusal reduction of the functional cusp, a 1.5-mm occlusal reduction of the non-functional cusp, a 1.0-mm shoulder finish line with a rounded inner edge, and a convergence angle of approximately 6° (Figure 5 c, d).



Figure 4. Melamine formaldehyde resin tooth model.

Table 4. Materials used in the study.

Materials	Product name	Contents	Manufacture
Zirconia	C-Pro Nano-Zirconia	ZrO ₂ , Al ₂ O ₃ , CeO ₂	Panasonic Healthcare
Artificial tooth	Simple Root Tooth Model A50A-500	Melamine formaldehyde resin	Nissin
Impression material	Omnidoble	Hydrophilic vinyl polysiloxane	Omnident
Wax	Thowax	Compound of microcrystalline and paraffin hydrocarbon waxes, natural waxes, resin and ester waxes	Yeti
Investment material	GC Fujivest Premium	Crystalline Silica 20-50%, Diammonium Hydrogen Orthophosphate 5-10%	GC Eupore
Co-Cr alloy	StarLoy C	Co 59.4%, Cr 24.5%, Wolfram (W) 10.0%, Niobium (Nb) 2.0%, Silicium (Si) 1.0%, Molybdenum (Mo) 1.0%, Iron (Fe) 0.1%	DeguDent
Cement	RelyX Unicem 2	Base paste; Methacrylate monomers containing phosphoric acid groups, Silanated fillers, Initiator components, Stabilizers, Rheological additives Catalyst paste; Methacrylate monomer, Alkaline fillers, Silanated fillers, Initiator components, Stabilizers, Rheological additives, Pigments	3M ESPE
Resin tooth analog	Technovit 4000	Powder; Quartz (SiO ₂) > 90%, Dibenzoyl peroxide 0-5%, Dicyclohexyl phthalate 0-5% Liquid; Longer methacrylate 50-75%, Methyl methacrylate 25-50%, Styrene 5-10%, N,N-dimethyl-p-toluidine < 1%	Heraeus Kulzer

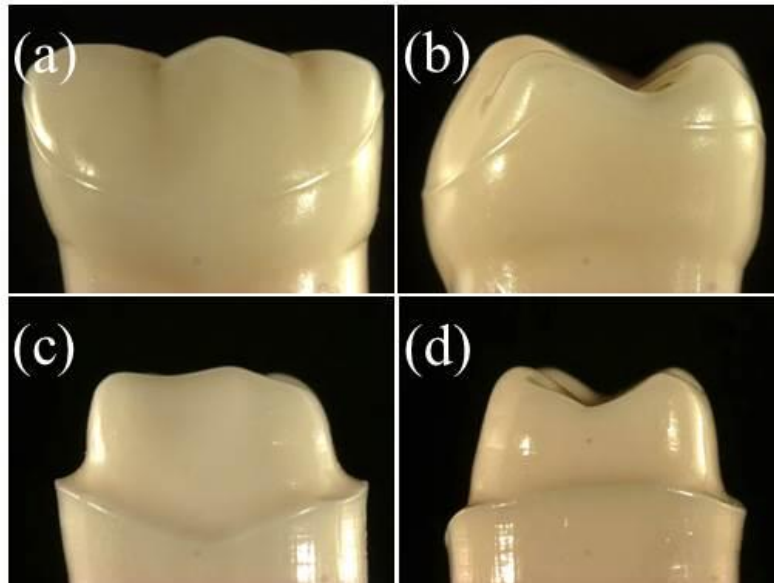


Figure 5. Abutment tooth preparation for all-ceramic crown (a, b, before preparation; c, d, after preparation).

2.1.2 Manufacturing of metal tooth analogs

To scan tooth information for subsequent veneering of porcelain on the zirconia framework, metal tooth analogs were replicated from the prepared artificial abutment tooth by taking an impression with hydrophilic vinyl polysiloxane impression material (Omnidouble, Omnident Dental-Handelsgesellschaft GmbH, Rodgau Nieder-Roden, Germany). A milling wax (Thowax gray opaque, Yeti Dental GmbH, Engen, Germany) was flowed into the impression, and a wax-up was made (Figure 6). The wax-up was invested with carbon-free phosphate-bonded investment material (GC Fujivest Premium, GC Eupore N.V., Leuven, Belgium), and cast using cobalt-chrome (Co-Cr) alloy (StarLoy C, DeguDent GmbH, Hanau, Germany) with a casting machine (Nautilus CC-plus, BEGO GmbH, Bremen, Germany) (Figure 7). After casting, Co-Cr tooth analogs were adjusted and polished (Figure 8).

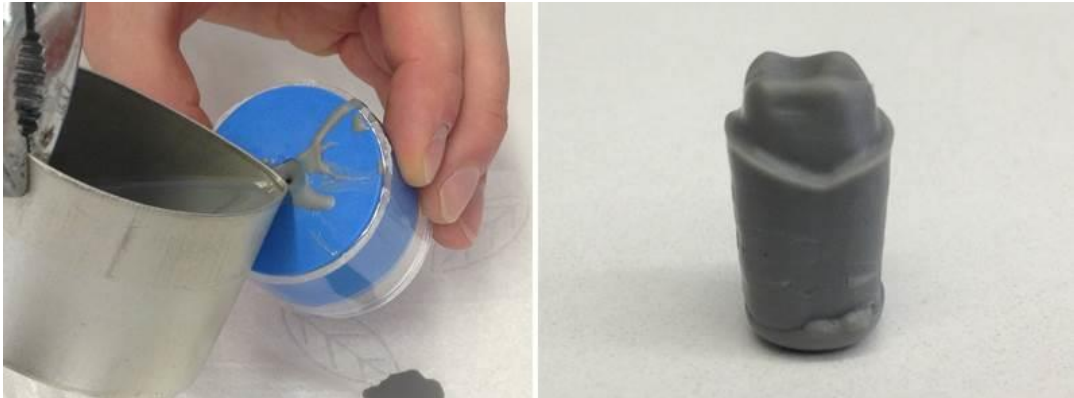


Figure 6. Wax-up of the prepared abutment tooth.



Figure 7. Casting machine.



Figure 8. Co-Cr tooth analog.

2.1.3 CAD/CAM process

Zirconia frameworks were made of Ce-TZP/A blanks (C-Pro Nano-Zirconia, Panasonic Healthcare Co., Ltd., Tokyo, Japan) (Figure 9) using a CAD/CAM system (C-Pro System, Panasonic Healthcare Co., Ltd.).



Figure 9. Ce-TZP/A blanks.

The Co-Cr tooth analog was coated with antireflection spray (CEREC Optispray, Sirona Dental GmbH, Salzburg, Austria) and scanned with a digital scanner (D700-3SP Scanner, Panasonic Healthcare Co., Ltd.) to obtain information for the prepared abutment tooth (Figure 10). After scanning, a zirconia framework was designed by a software (3Shape Dental Designer, 3Shape A/S, Copenhagen, Denmark) and milled using a Ce-TZP/A blank (Figure 11).



Figure 10. Digital scanner.

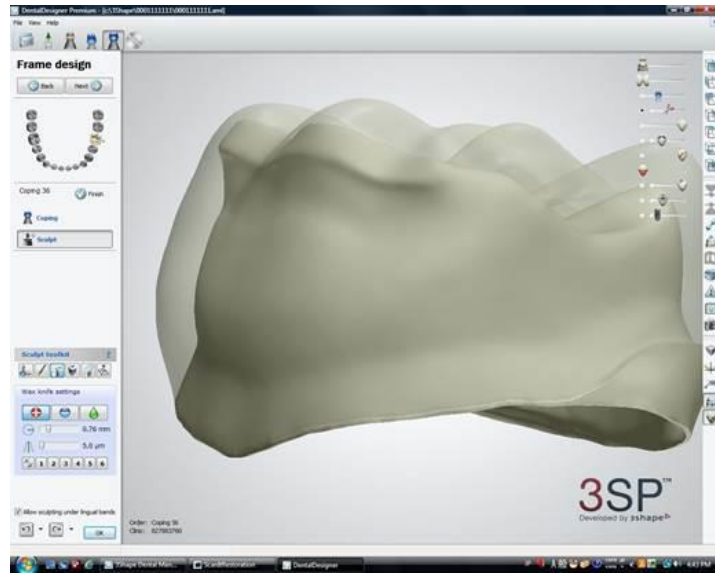


Figure 11. Framework design by a CAD software.

2.1.4 Fabrication of Ce-TZP/A frameworks

The four different zirconia framework designs (n = 96) used in this study are as follows (Figure 12, Table 5):

Group 1: Standard framework design; 0.3-mm framework thickness with an anatomical occlusal shape.

Group 2: Modified framework design of the occlusal anatomical shape, with an added framework thickness of 1.0 mm on the lingual margin and a height of 2.0 mm (lingual supporting structure).

Group 3: Modified framework design of the occlusal anatomical shape, with an added framework thickness of 0.5 mm at the external surface of the buccal cusp (buccal supporting structure).

Group 4: Modified framework design with an anatomical occlusal shape and additional buccal and lingual supporting structures (Figure 13).

After the milling process, the pre-sintered Ce-TZP/A frameworks were sintered according to the manufacturer's instructions.

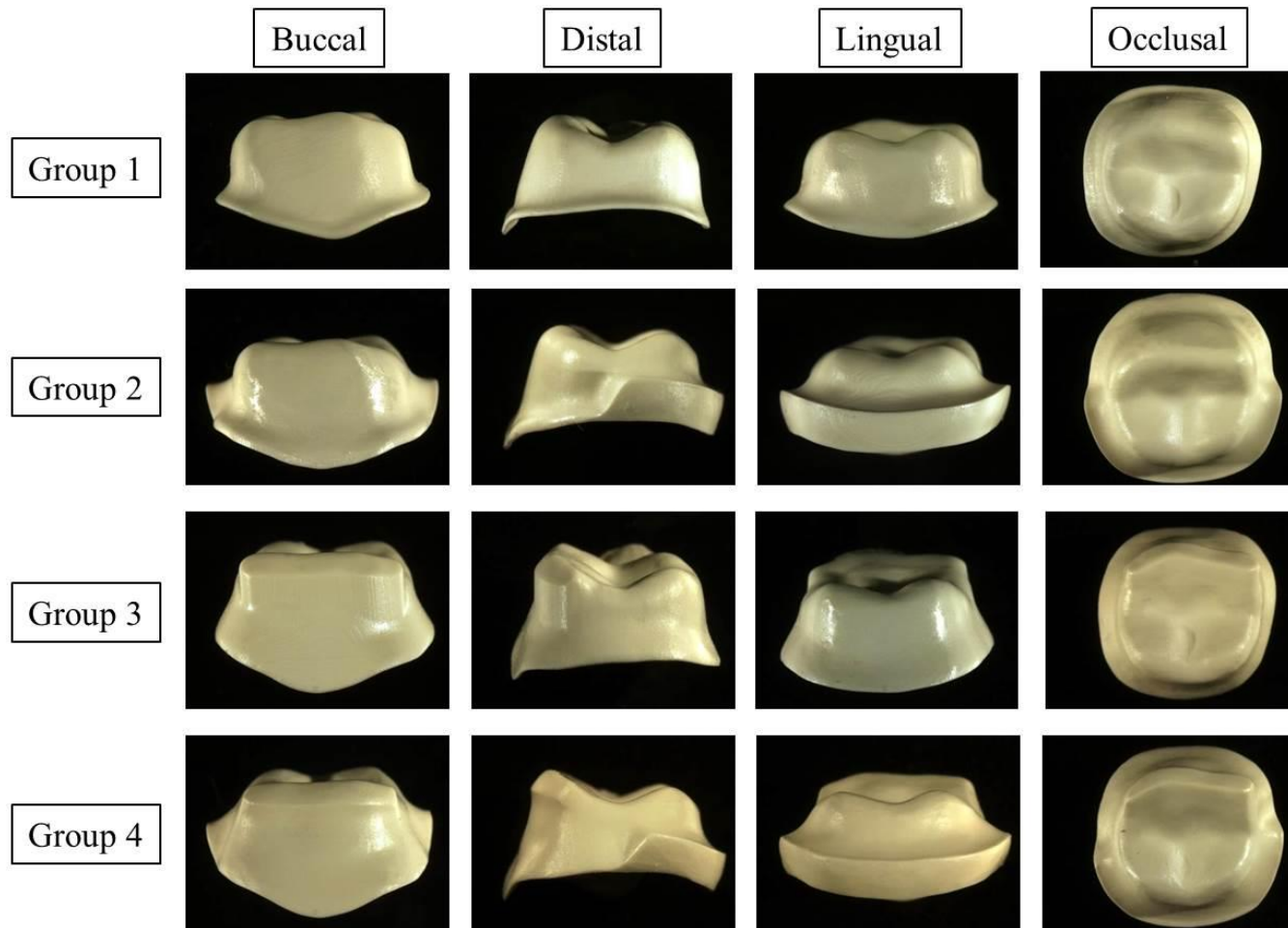


Figure 12. Ce-TZP/A frameworks. Group 1, occlusal anatomical shape; Group 2, with an additional lingual supporting structure; Group 3, with an additional buccal supporting structure; Group 4, with additional buccal and lingual supporting structures.

Table 5. Experimental groups.

Group	Framework design	Condition	Number
1 (-)	Occlusal anatomical shape	Immersed in distilled water for 24 h 37° C	12
1 (+)		with chewing simulation (1.2 million cycles)	12
2 (-)	With additional lingual supporting structure	Immersed in distilled water for 24 h 37° C	12
2 (+)		with chewing simulation (1.2 million cycles)	12
3 (-)	With additional buccal supporting structure	Immersed in distilled water for 24 h 37° C	12
3 (+)		with chewing simulation (1.2 million cycles)	12
4 (-)	With additional buccal and lingual supporting structures	Immersed in distilled water for 24 h 37° C	12
4 (+)		with chewing simulation (1.2 million cycles)	12

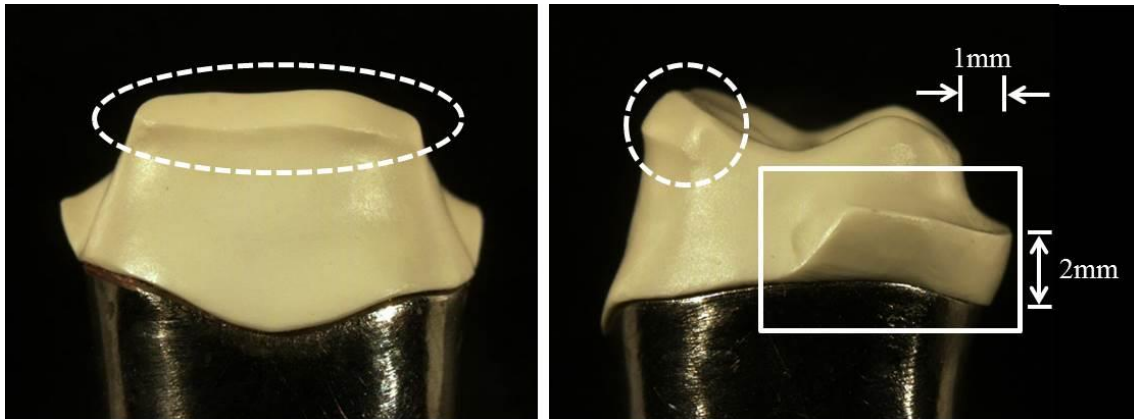


Figure 13. Supporting structures. Dotted areas and solid area indicate buccal and lingual supporting structures, respectively.

2.2 Veneering porcelain on Ce-TZP/A framework

Each sintered Ce-TZP/A framework was veneered with feldspathic ceramics via conventional layering technique to fabricate an all-ceramic crown.

2.2.1 Pretreatment of framework surface

The surfaces of Ce-TZP/A frameworks were blasted with 50 μm Al_2O_3 particles (Spezial-Edelkorund Klasse 30B/50my, Harnisch & Rieth GmbH, Winterbach, Germany) with an airborne-particle abrasion device (P-G 400, Harnisch & Rieth GmbH) under 0.2 MPa pressure for 10 sec. The distance between the nozzle and the framework surface was 10 mm vertically. All frameworks were cleaned with ethanol followed by distilled water in an ultrasonic device (SONOREX SUPER RK102 H, Bandelin GmbH, Berlin, Germany) for 10 min, then dried.

2.2.2 Layering process

The layering procedure comprised the following: wash-bake (VITA VM9 Effect Liner EL, VITA Zahnfabrik H. Rauter GmbH & Co. KG, Bad Säckingen, Germany); first and second dentin (VITA VM9 Base Dentin A3, VITA Zahnfabrik H. Rauter GmbH & Co. KG); and glazing (VITA Akzent, VITA Zahnfabrik H. Rauter GmbH & Co. KG), which was performed in a dental furnace (Austromat 624, Dekema Dental-Keramiköfen GmbH, Freilassing, Germany) according to the manufacturer's instructions (Figure 14, Table 6).



Figure 14. Dental porcelain furnace.

Table 6. Time schedule of porcelain firing.

Firing steps	Product name	Dry (min)	Close (min)	Pre-Heating (° C)	Heating rate (° C/min)	Firing (° C)	Holding time (min)	Vaccum time (min)
Liner	VM9 EFFECT LINER EL4	3	3	500	55	930	1	7.49
Dentine 1	VM9 BASE DENTINE A3	3	3	500	55	910	1	7.27
Dentine 2	VM9 BASE DENTINE A3	3	3	500	55	900	1	7.16
Glaze	VITA AKZENT	2	2	500	80	900	1	-

Before wash-bake firing (Figure 15), molds for reproduction of the tooth form before tooth preparation (Figure 5 a, b) were made using impression material (FUSION II Putty Type, GC Co., Ltd., Tokyo, Japan) for layering porcelain on the Ce-TZP/A framework. In brief, a resin-up replica crown for each framework was made using a self-curing modelling acrylic (Palavit G, Heraeus Kulzer GmbH, Hanau, Germany) (Figure 16 a). This replica crown was fixed on the Co-Cr tooth analog, and an impression was taken (Figure 16 b, c). For the dentin layer, base dentin powder was mixed with the liquid and filled into the mold, which had been precoated with isolating liquid (Carat, Hager & Werken GmbH, Düisburg, Germany) (Figure 16 d, e). A tissue was used to remove excess moisture from the porcelain build-up on the Ce-TZP/A framework, and the framework was fired (Figure 16 f). Finally, a glazing firing was performed to fabricate all-ceramic crowns using a Ce-TZP/A framework (Figure 17).

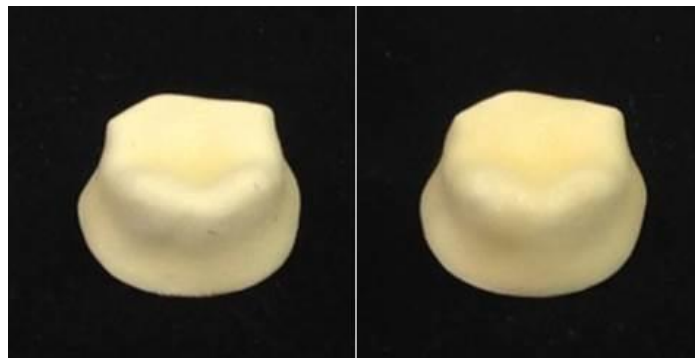


Figure 15. Ce-TZP/A framework after wash-bake firing (left, first firing; right, second firing).

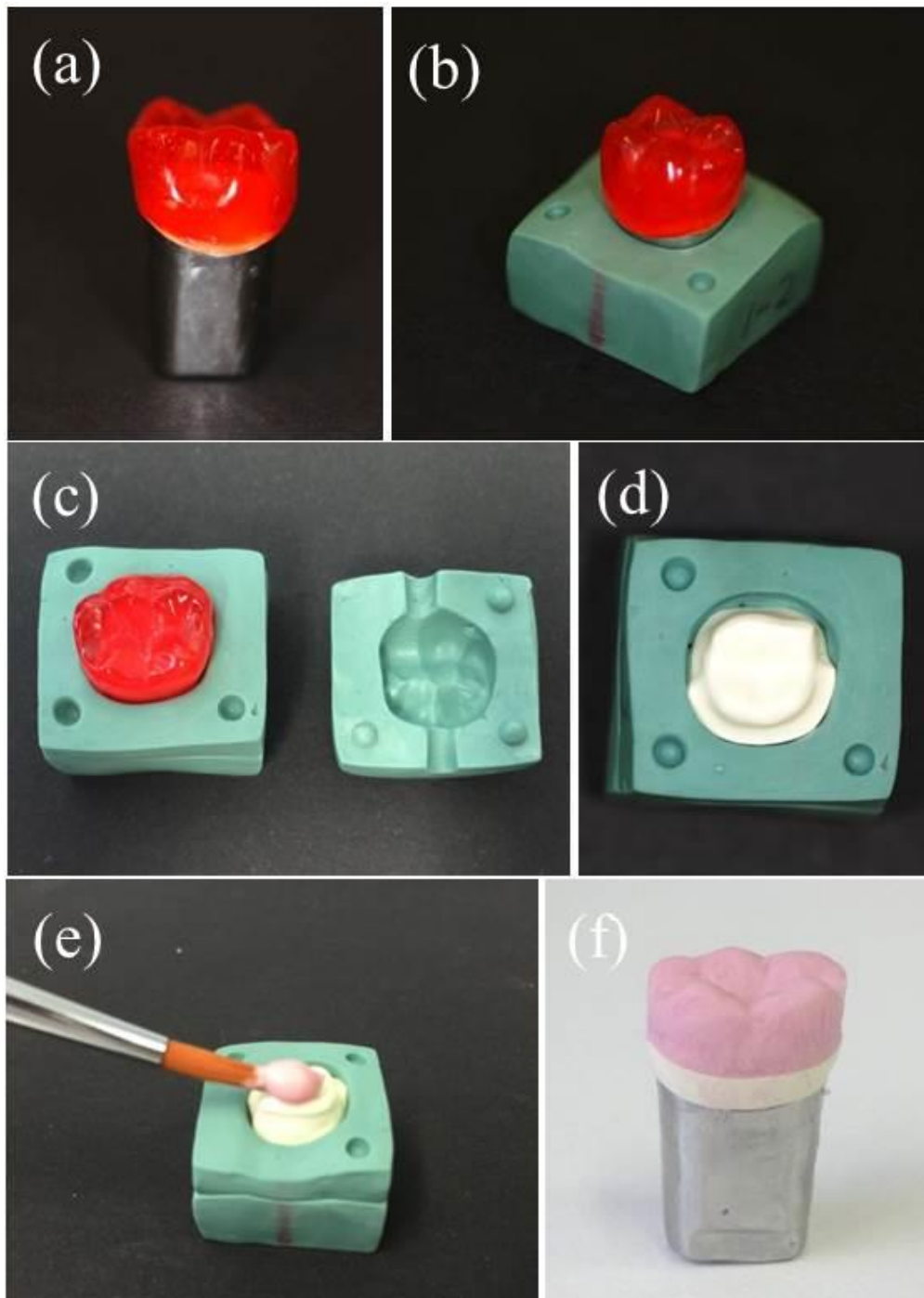


Figure 16. Process of veneering porcelain. (a, fabrication of a resin-up replica crown for each framework; b, c, fabrication of mold ; d, fixation of framework; e, layering porcelain on the framework; (f) build-up of porcelain.



Figure 17. Ce-TZP/A-based all-ceramic crown after glazing firing.

2.3 Cementation of Ce-TZP/A based crowns

Resin tooth analogs, to which Ce-TZP/A-based crowns would be cemented, were made from cold polymerizing resin. Before cementation, the outer and inner surfaces of resin tooth analogs and Ce-TZP/A crowns, respectively, were sandblasted. Treated Ce-TZP/A-based crowns were then cemented to resin tooth analogs using self-adhesive resin cements. After cementation, all specimens were stored in distilled water for 24 h at 37° C.

2.3.1 Manufacturing of resin tooth analogs

Resin tooth analogs were made from a fast-curing resin that was based on modified polyester (Technovit 4000, Heraeus Kulzer) (Figure 18). In brief, an impression of the prepared abutment tooth (Figure 5 c, d) was taken with hydrophilic vinyl polysiloxane impression material (Omnidouble, Omnident Dental-Handelsgesellschaft GmbH). Resin powder was mixed with liquid according to the manufacturer's instructions, then flowed into the impression and polymerized. After polymerization, resin tooth analogs were stored in distilled water for 24 h at 37° C.



Figure 18. Resin tooth analog.

2.3.2 Pretreatment of resin tooth analog surfaces

The surfaces of the resin tooth analogs were sandblasted as described above. All resin tooth analogs were cleaned with ethanol and distilled water in an ultrasonic device, then dried.

2.3.3 Pretreatment of crown inner surfaces

The inner surfaces of Ce-TZP/A based crowns were sandblasted as described above, according to the manufacturer's instructions. All crowns were then cleaned and dried.

2.3.4 Cementation of Ce-TZP/A based crowns

After pretreatment, all crowns were cemented to resin tooth analogs using self-adhesive resin cement (RelyX Unicem 2, 3M ESPE GmbH, Neuss, Germany). In this study, this dual-cure cement was cured by chemical polymerization. During this procedure, all specimens were held with 1 kg of weight applied to the top of the crown with a 4-mm stainless steel ball for 6 min using an original loading device (Figure 19). Excess cement was removed after 2.5 min during cementation. All cemented specimens were stored in distilled water for 24 h at 37° C.



Figure 19. Original loading device for cementation of Ce-TZP/A-based crowns.

2.4 Fixation

2.4.1 Manufacturing of acrylic disk blocks

Acrylic disk blocks (φ 30 mm \times 0.8 mm, $n = 96$) were made from a self-curing modelling acrylic (Palavit G, Heraeus Kulzer GmbH). Holes were drilled in the middle of these blocks to fix the specimens.

2.4.2 Fixation of the specimens to acrylic disk blocks

Each specimen was embedded in an acrylic block, positioned using an original loading device such that the long axis of the tooth was 2.0 mm below the margin line (Figure 20). Fixed specimens were stored in distilled water for 24 h at 37° C.

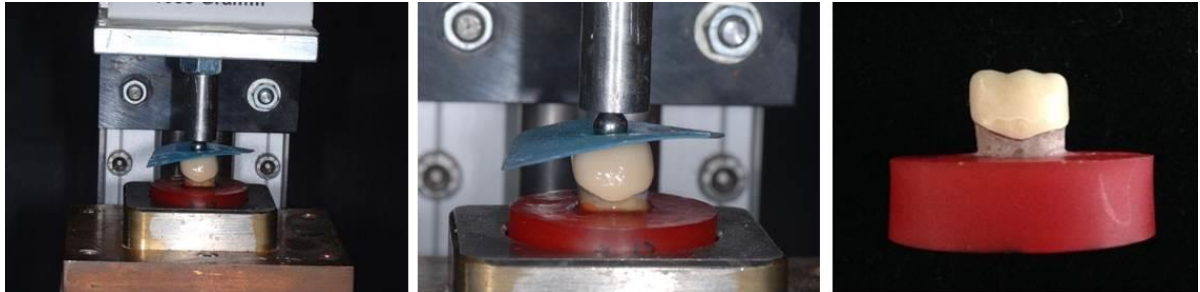


Figure 20. Fixation of a specimen to an acrylic disk block.

2.5 Mechanical preloading by chewing simulation

Prior to fracture loading test, half of the specimens in each experimental group ($n = 12$) underwent mechanical preloading. Specimens were mounted into a metal holder, and mechanical preloading was conducted using a masticator (Willytec, SD Mechatronik GmbH, Feldkirchen-Westerham, Germany). The loading simulation, which was supposed

to represent 5 years of oral service, used the following parameters (Rosentritt et al, 2009): weight, 49 N; cycles, 1.2 million; frequency, 1.4 Hz; and speed, 40 mm/s (Figure 21). The antagonist used material comprising 5-mm magnesium silicate balls (Steatite, CeramTec GmbH, Plochingen, Germany). The antagonist was placed at the occlusal surface of each crown, and adjustments were made using red articulating paper and vertical-centric loading to confirm three-point contact (Figure 22).



Figure 21. Masticator.



Figure 22. Antagonist (left) and three-point contact with the fixed specimen (right).

2.6 Fracture loading test

Fracture load of each crown, either without (-) or with (+) chewing simulation, was conducted using a universal testing machine (Z010, Zwick GmbH, Ulm, Germany) (Figure 23). The crown was mounted into the metal holder. Using a 4.0-mm stainless steel ball as a loading rod tip, a vertical load was then applied at the central fossa of each crown at a crosshead speed of 0.5 mm/min until fracture occurred (Figure 24).



Figure 23. Universal testing machine.



Figure 24. Fracture loading test.

2.7 Analysis of failure mode

After fracture loading test, failure mode of each crown was observed by stereomicroscopy (M400 Photomicroscope, Wild Heerbrugg AG, Heerbrugg, Switzerland) and scanning electron microscopy (SEM; LEO 1430, Carl Zeiss AG, Oberkochen, Germany) (Figure 25, 26).



Figure 25. Stereomicroscopy.

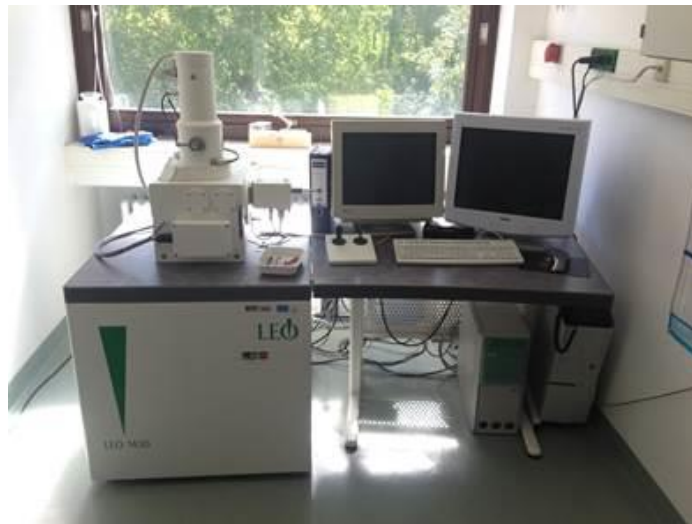


Figure 26. Scanning electron microscopy.

Failure mode was classified into two groups: partial fracture (cracking or chipping of porcelain veneer) and complete fracture (fracture of Ce-TZP/A framework or tooth analog) (Table 7, Figure 27).

Table 7. Classification of failure modes.

(1) Partial fracture	<ul style="list-style-type: none">• Cracking of porcelain veneer• Chipping of porcelain veneer
(2) Complete fracture	<ul style="list-style-type: none">• Fracture of Ce-TZP/A framework• Fracture of tooth analog

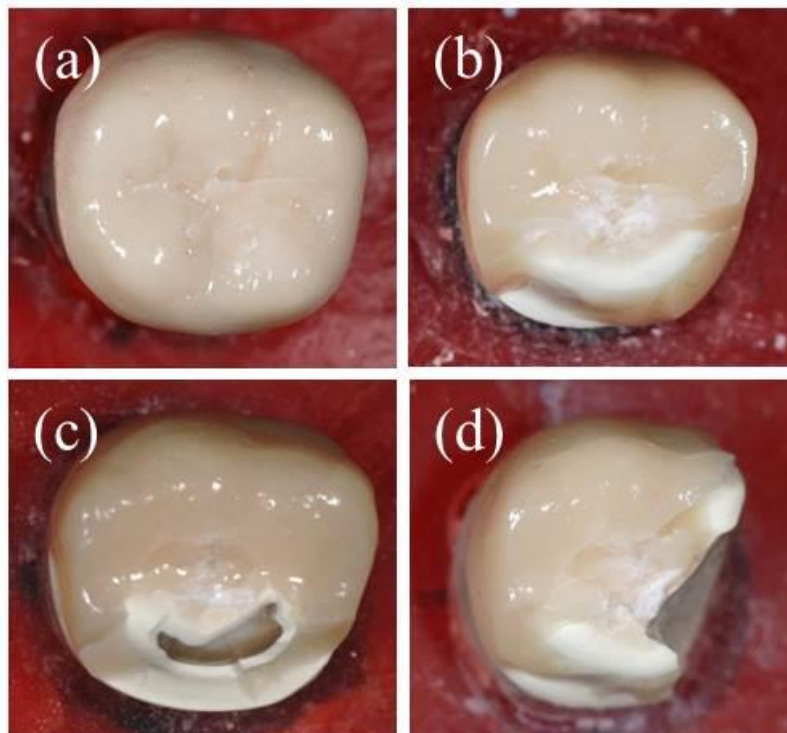


Figure 27. Failure mode classification. Partial fracture: cracking of porcelain veneer (a) and chipping of porcelain veneer (b). Complete fracture: fracture of Ce-TZP/A framework (c) and fracture of tooth analog (d).

2.8 Statistical analysis

Fracture load results were analyzed by two-way analysis of variance (ANOVA) with framework design and mechanical preloading as independent factors followed by the Scheffe's test for post-hoc comparisons ($\alpha = 0.05$). For the purpose of statistical analysis, prefailure after mechanical preloading was included as complete fracture. The failure modes' results were analyzed by the Fisher's exact test. The statistical analyses were performed by the software packages (Excel Statistics 2010, Social Survey Research Information Co., Ltd., Tokyo, Japan; R version 3.2.3, The R Foundation for Statistical Computing, Vienna, Austria).

3.0 Results

3.1 Chewing simulation

Attrition marks due to contact with the antagonist during chewing simulation were found in each experimental group subjected to mechanical preloading.

After mechanical preloading, prefailure occurred only in Group 1(+), in which three crowns (25%) exhibited cracking or chipping of veneering porcelain (Figure 28). These crowns were excluded from subsequent fracture load.

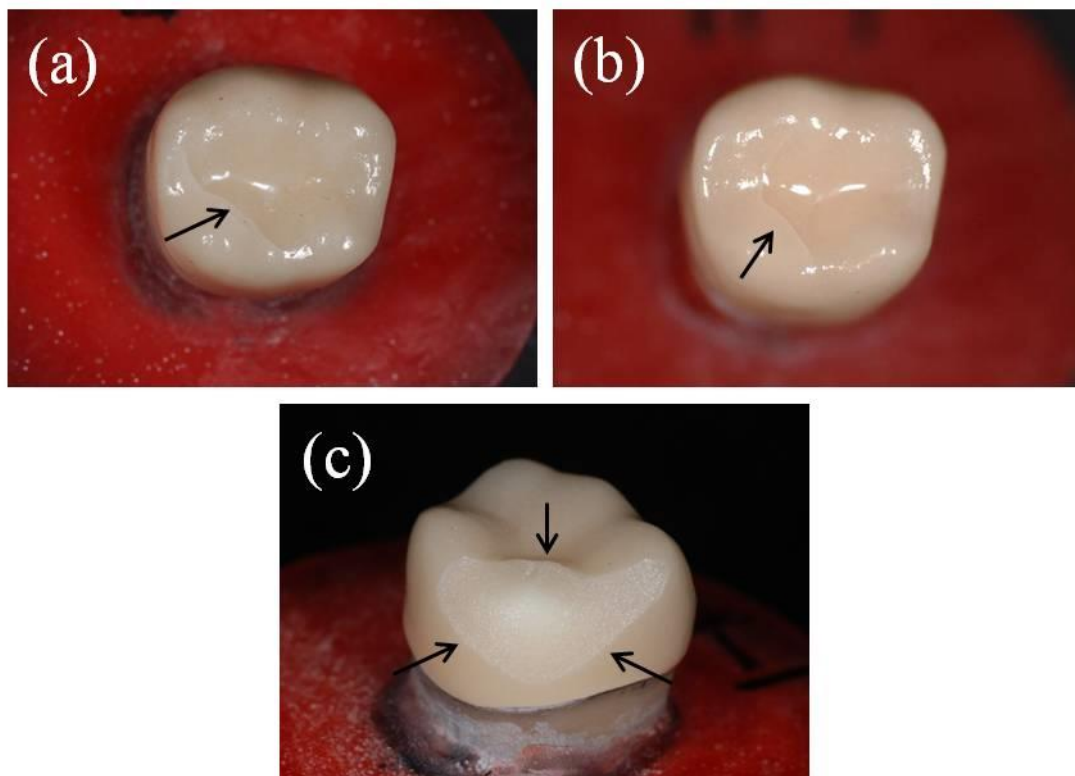


Figure 28. Photographs of prefailure after mechanical preloading in Group 1(+). Cracking of porcelain veneer (a, b); chipping of porcelain veneer (c). Black arrows indicate fracture lines.

3.2 Fracture load

Fracture load in each experimental group is shown in Figures 29–31 and Table 8.

Fracture load ranged from 1866 ± 262 N (Group 3(-)) to 2049 ± 430 N (Group 1(-)) in the experimental groups without mechanical preloading (Figure 29). There was no significant difference in fracture loads between groups not subjected to mechanical preloading.

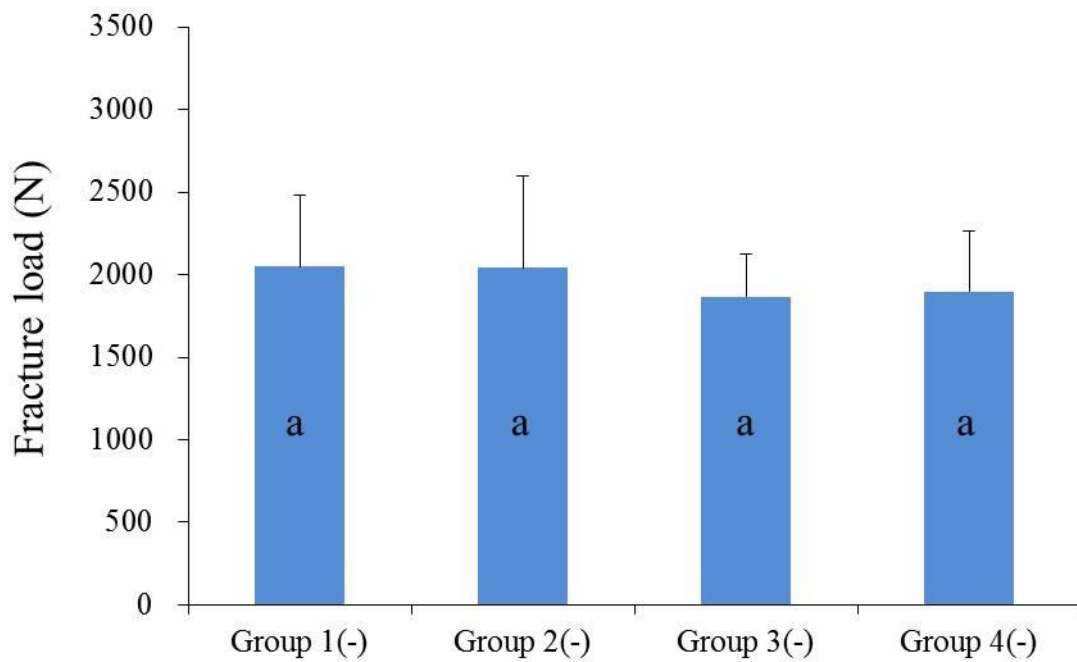


Figure 29. Fracture load in experimental groups without mechanical preloading. Groups labeled with the same letter are not statically different ($p > 0.05$).

Conversely, fracture load ranged from 1828 ± 374 N (Group 1(+)) to 2374 ± 464 N (Group 2(+)) in the experimental group with mechanical preloading (Figure 30). Fracture load was significantly higher in Group 2(+) than in Group 1(+) ($p < 0.05$); however, no significant difference was found between Groups 2(+) and 3(+), and Groups 2(+) and 4(+).

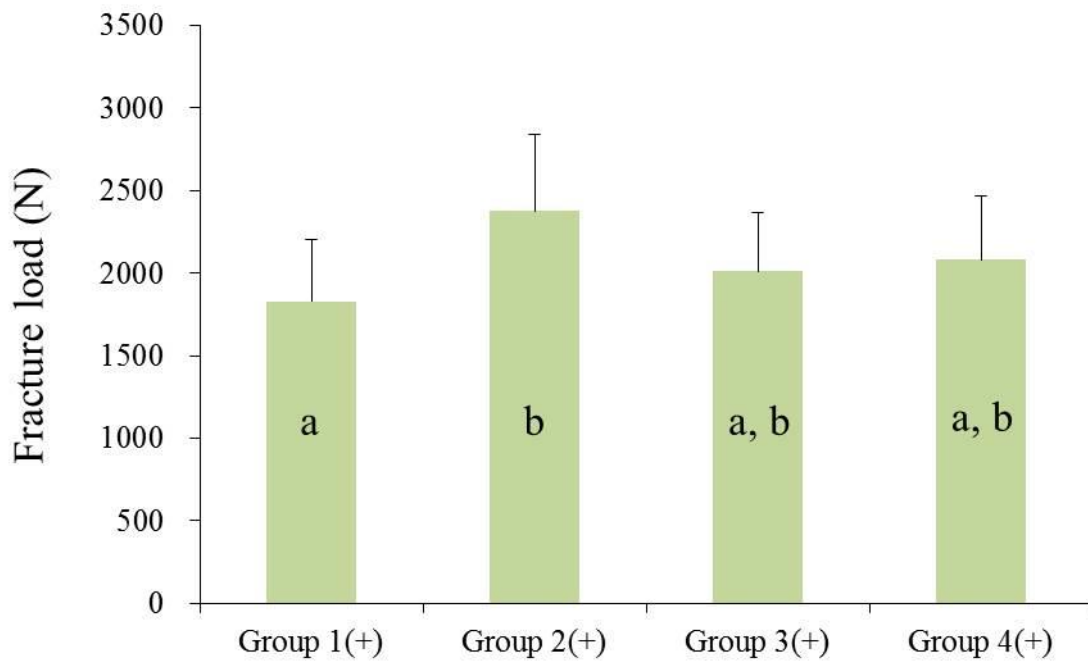


Figure 30. Fracture load in experimental groups with mechanical preloading. Groups labeled with different letters are statically different ($p < 0.05$).

In the chewing simulation, fracture load tended to decrease after mechanical preloading in frameworks with no additional supporting structure (Group 1), but tended to increase in frameworks with additional supporting structures (Groups 2, 3, and 4) (Figure 31).

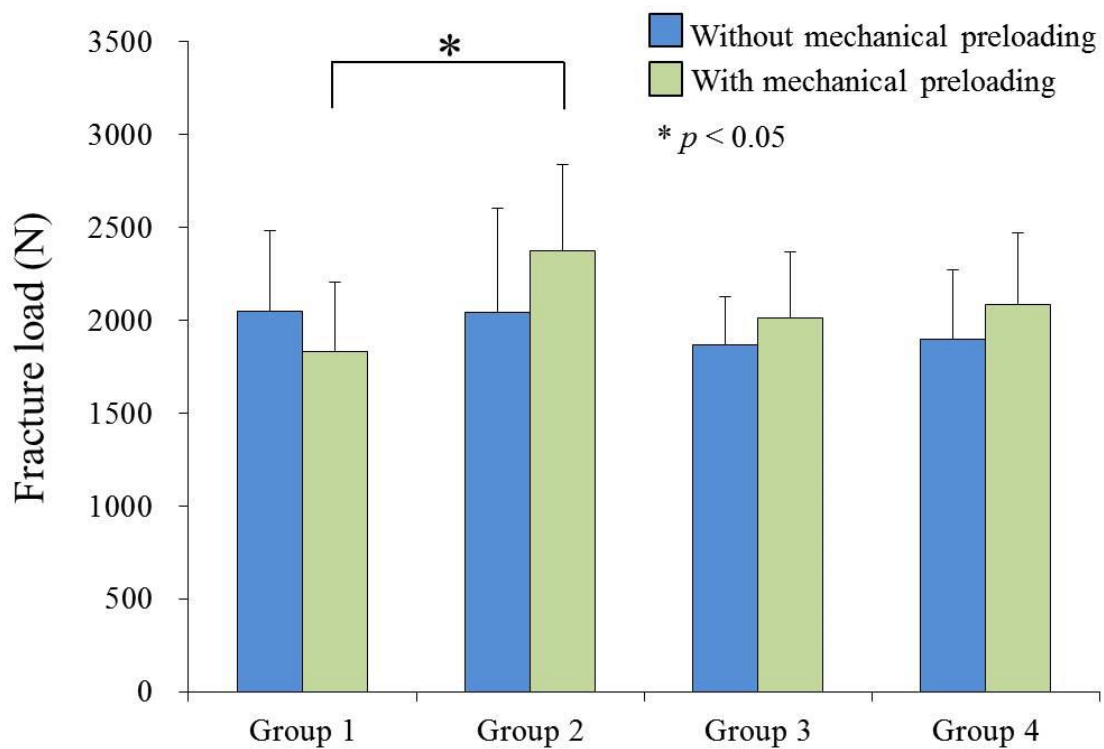


Figure 31. Comparison of the fracture load results after chewing simulation in each experimental group. The asterisk indicates statistical significance ($p < 0.05$).

Table 8. Fracture loads (N) of all-ceramic crowns using different Ce-TZP/A frameworks (mean \pm SD).

Experimental group	Mean \pm SD (N)	
	Without mechanical preloading (-)	With mechanical preloading (+)
Group 1	2049 \pm 430 ^A _a	1828 \pm 374 ^A _a
Group 2	2040 \pm 562 ^A _a	2374 \pm 464 ^A _b
Group 3	1866 \pm 262 ^A _a	2009 \pm 360 ^A _{a,b}
Group 4	1897 \pm 371 ^A _a	2081 \pm 387 ^A _{a,b}

Note: Results of statistical analysis are represented by upper and lower case letters. Different uppercase letters in the same row mean that the groups are significantly different ($p < 0.05$). Different lowercase letters in the same column mean that the groups are significantly different ($p < 0.05$). Group 1, occlusal anatomical shape; Group 2, with additional lingual supporting structure; Group 3, with additional buccal supporting structure; Group 4, with additional buccal and lingual supporting structures.

3.3 Failure mode

3.3.1 Failure mode description

Classification of failure modes by stereomicroscopy and SEM for each experimental group is shown in Table 9 and Figures 32–41, respectively.

After fracture loading test, one partial fracture type, cracking of porcelain veneer, was observed in all experimental groups except for Group 3(-). Three cases of cracking each occurred in Groups 1(-) and 2(-), and two cases each occurred in Groups 4(-) and 1–4(+)
(Figure 32 g, h). The cracked area was limited to the occlusal surface (Figure 37).

The major partial fracture, chipping of porcelain veneer, was also observed in all experimental groups, but differed in number: twelve cases of chipping occurred in Group 3(-) (Figure 32 e, f); 10 each in Groups 4(-) and 4(+) (Figure 33 g, h); nine in Group 1(-) (Figure 32 a, b); eight in Group 3(+); seven in Group 2(-); and five in Groups 1(+) and 2(+) (Figure 33 a, b). The chipped area was mainly on the lingual side (Figures 34, 36, 38, and 41).

Fracture of Ce-TZP/A framework was observed in Group 2 (Figure 32 c, d). Fracture rarely occurred between the mesiolingual and distolingual cusps (Figure 35). Furthermore, fracture of tooth analog was observed in Group 2(-) and Groups 1–3(+) (Figure 33 c, f). The fracture area was on the lingual side (Figures 39, 40).

Table 9. Number of failure modes of all-ceramic crowns using different Ce-TZP/A frameworks.

Experimental group	Prefailure		Partial fracture		Complete fracture	
	Cracking of porcelain	Chipping of porcelain	Cracking of porcelain	Chipping of porcelain	Fracture of framework	Fracture of tooth analog
1 (-)	-	-	3	9	0	0
1 (+)	2	1	2	5	0	2
2 (-)	-	-	3	7	1	1
2 (+)	0	0	2	5	1	4
3 (-)	-	-	0	12	0	0
3 (+)	0	0	2	8	0	2
4 (-)	-	-	2	10	0	0
4 (+)	0	0	2	10	0	0

Group 1, occlusal anatomical shape; Group 2, with additional lingual supporting structure; Group 3, with additional buccal supporting structure; Group 4, with additional lingual and buccal supporting structures.

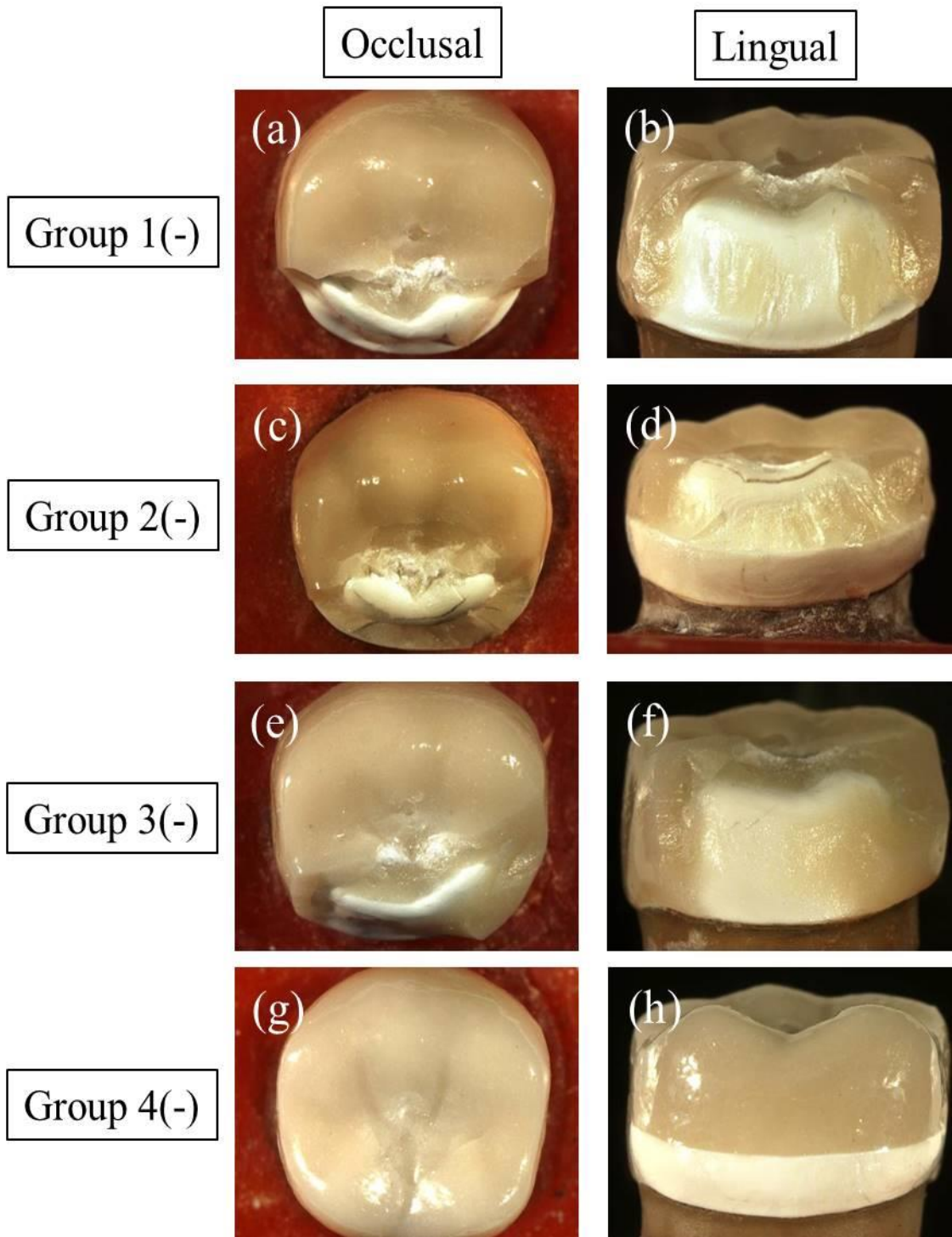


Figure 32. Stereomicroscopy of Ce-TZP/A crowns in Groups 1–4(-).

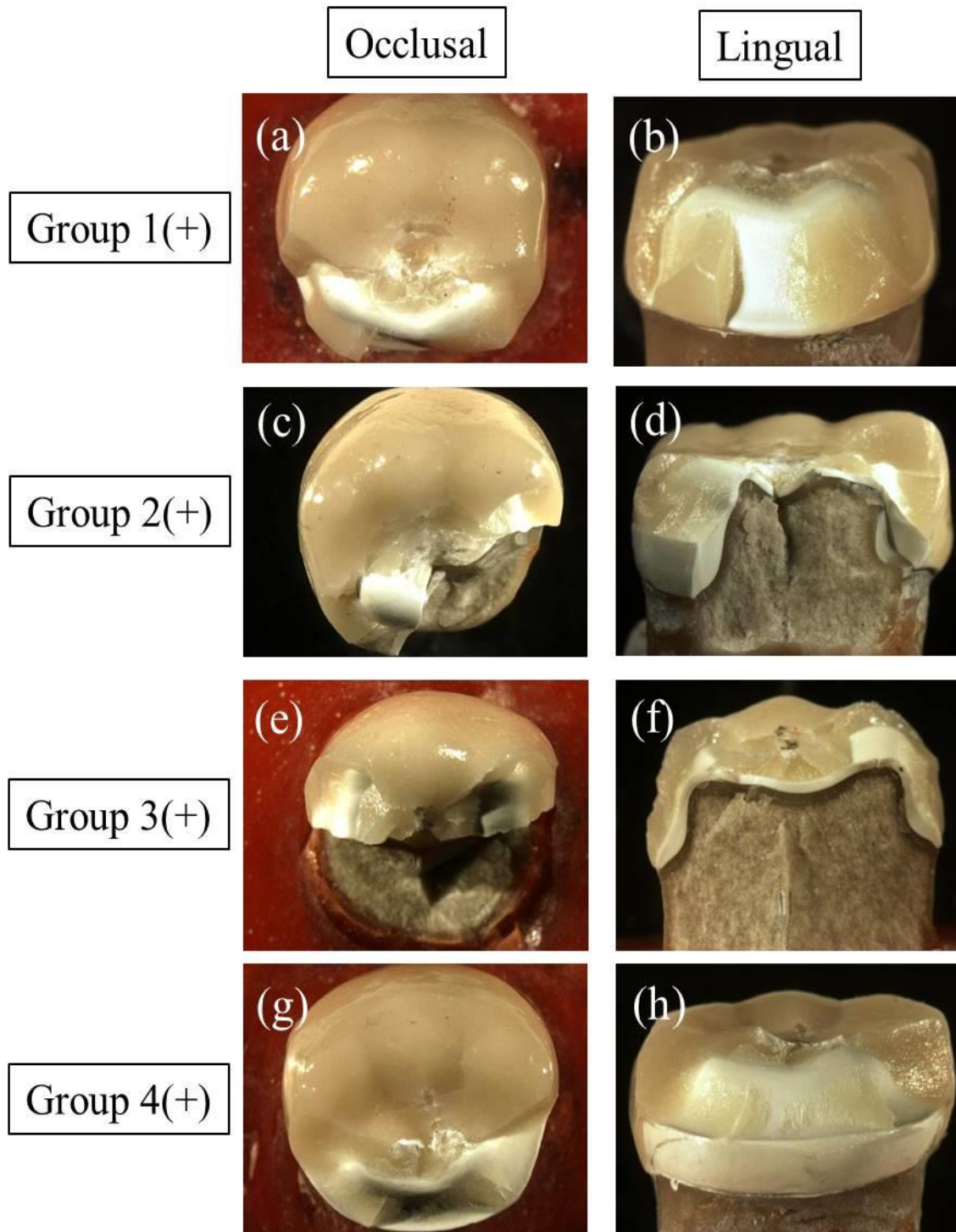


Figure 33. Stereomicroscopy of Ce-TZP/A crowns in Groups 1–4(+).

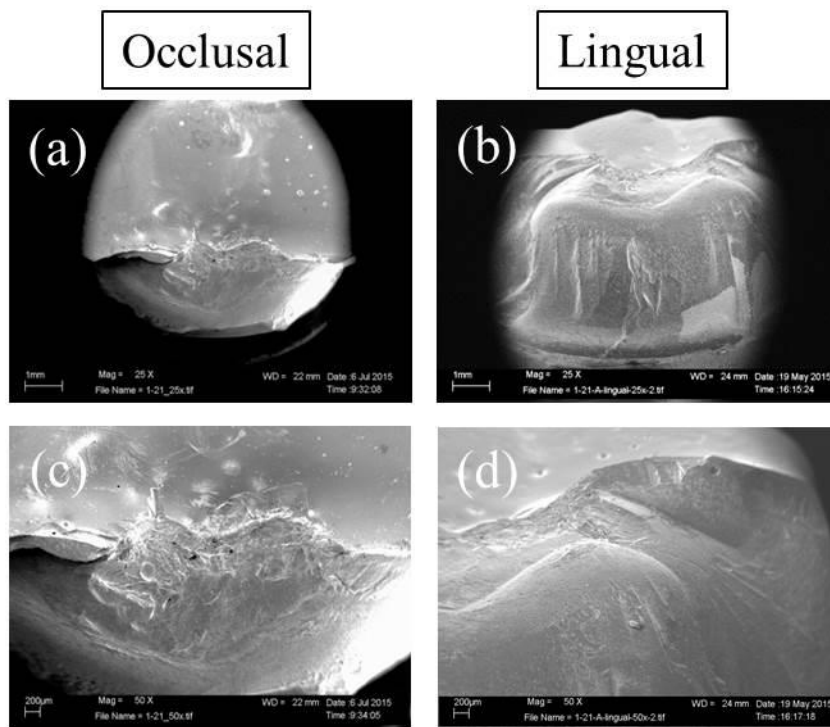


Figure 34. Scanning electron microscopy of Ce-TZP/A crown from Group 1(-). Magnification: a, b, 25×; c, d, 50×.

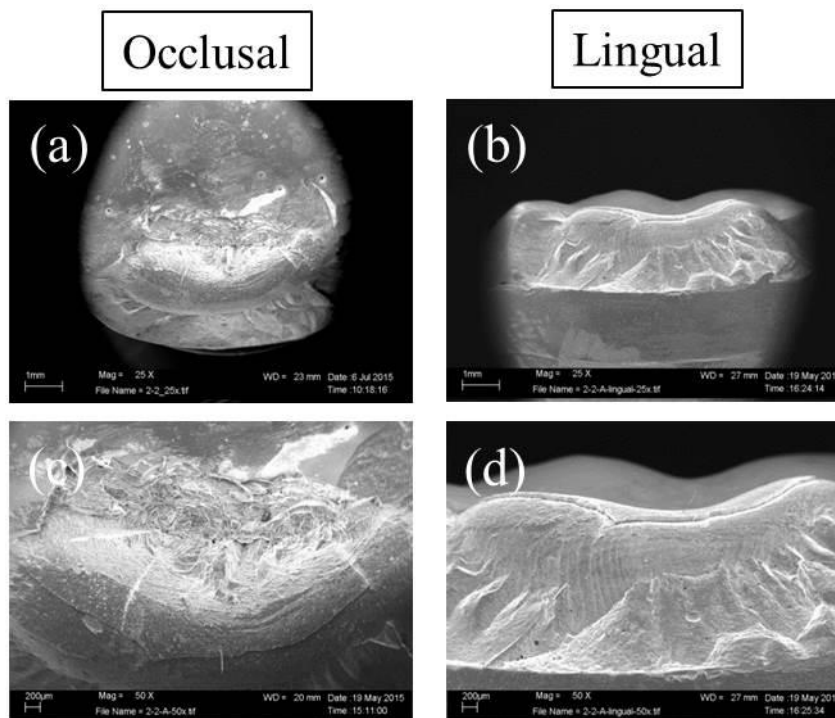


Figure 35. Scanning electron microscopy of Ce-TZP/A crown from Group 2(-). Magnification: a, b, 25×; c, d, 50×.

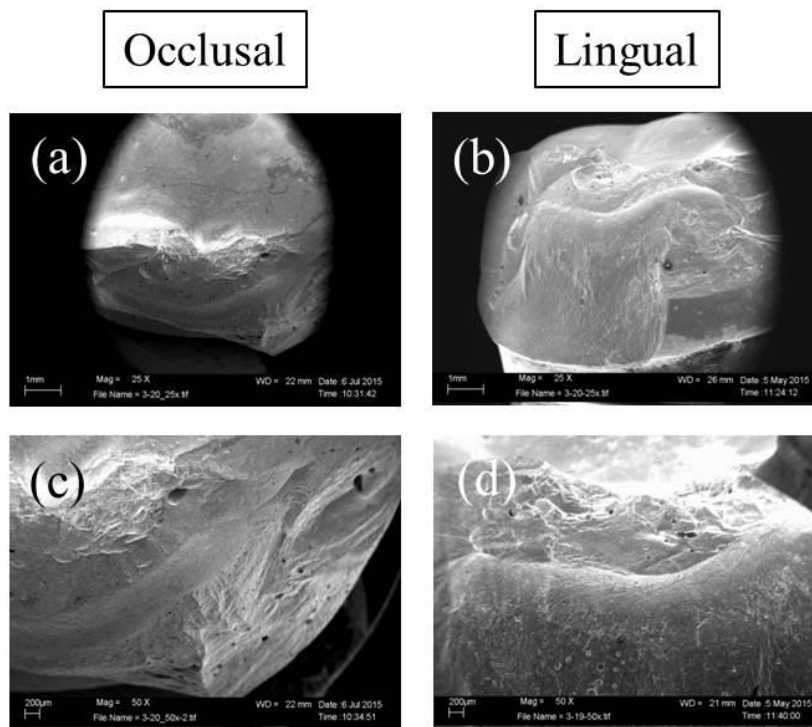


Figure 36. Scanning electron microscopy of Ce-TZP/A crown from Group 3(-). Magnification: a, b, 25 \times ; c, d, 50 \times .

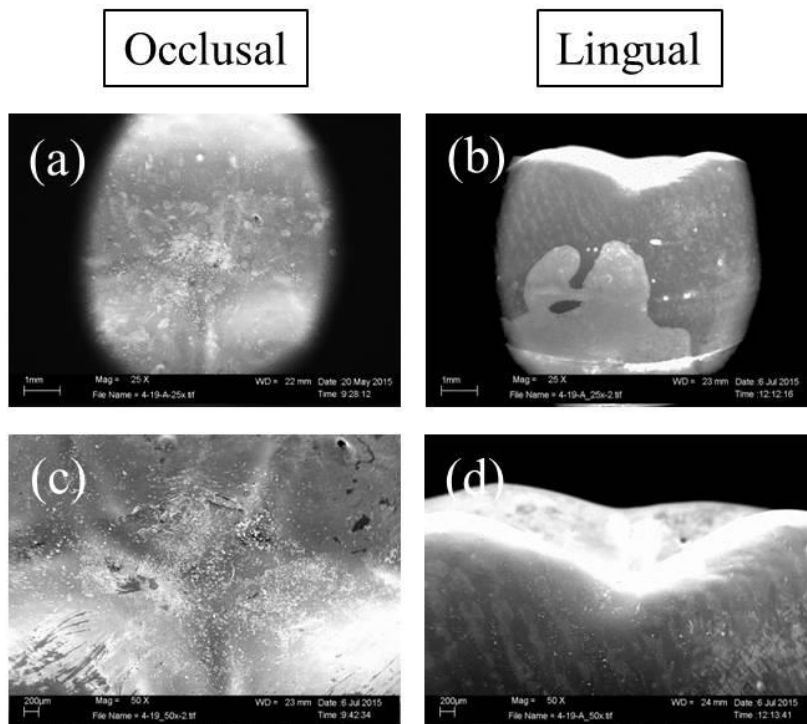


Figure 37. Scanning electron microscopy of Ce-TZP/A crown from Group 4(-). Magnification: a, b, 25 \times ; c, d, 50 \times .

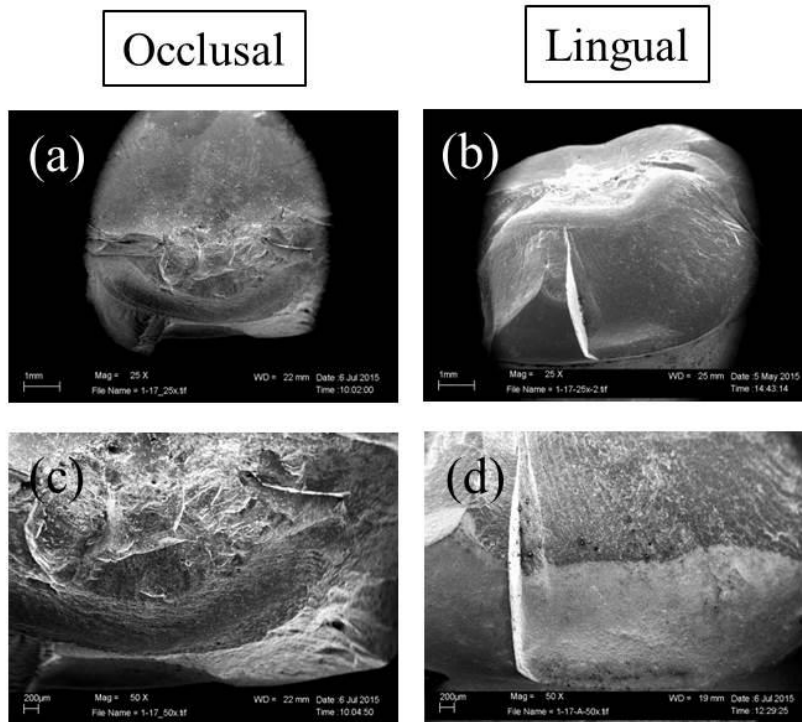


Figure 38: Scanning electron microscopy of Ce-TZP/A crown from Group 1(+).
Magnification: a, b, 25 \times ; c, d, 50 \times .

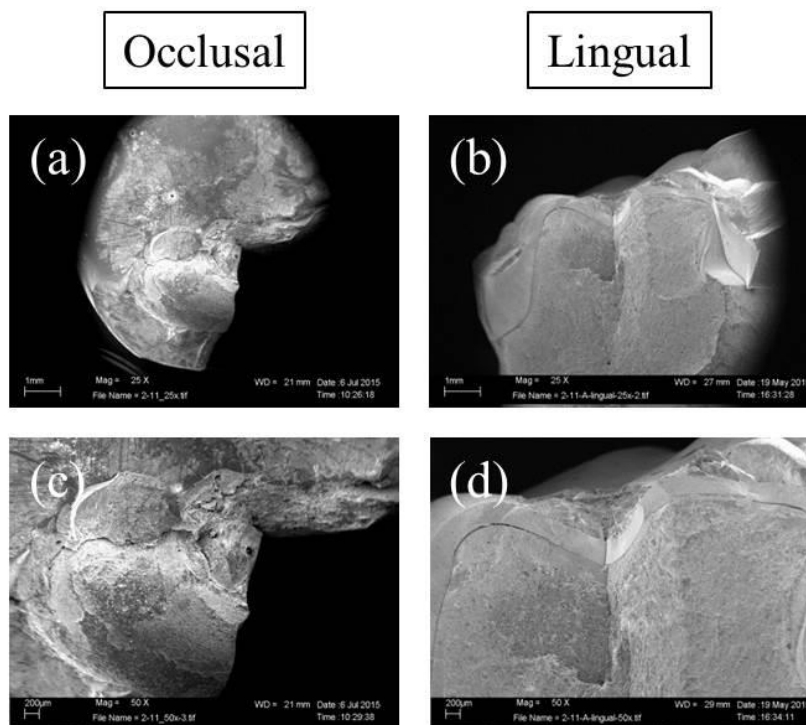


Figure 39. Scanning electron microscopy of Ce-TZP/A crown from Group 2(+).
Magnification: a, b, 25 \times ; c, d, 50 \times .

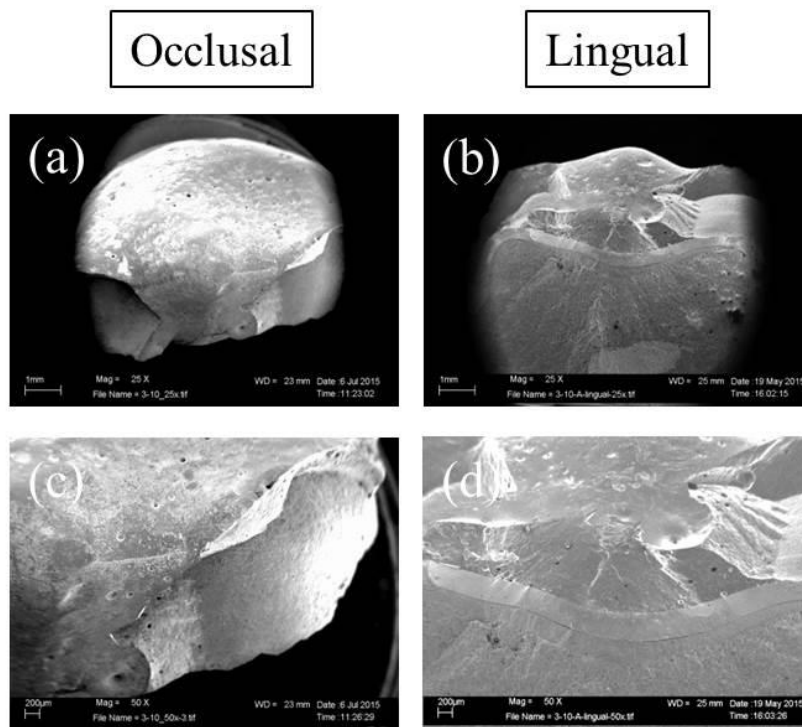


Figure 40. Scanning electron microscopy of Ce-TZP/A crown from Group 3(+). Magnification: a, b, 25 \times ; c, d, 50 \times .

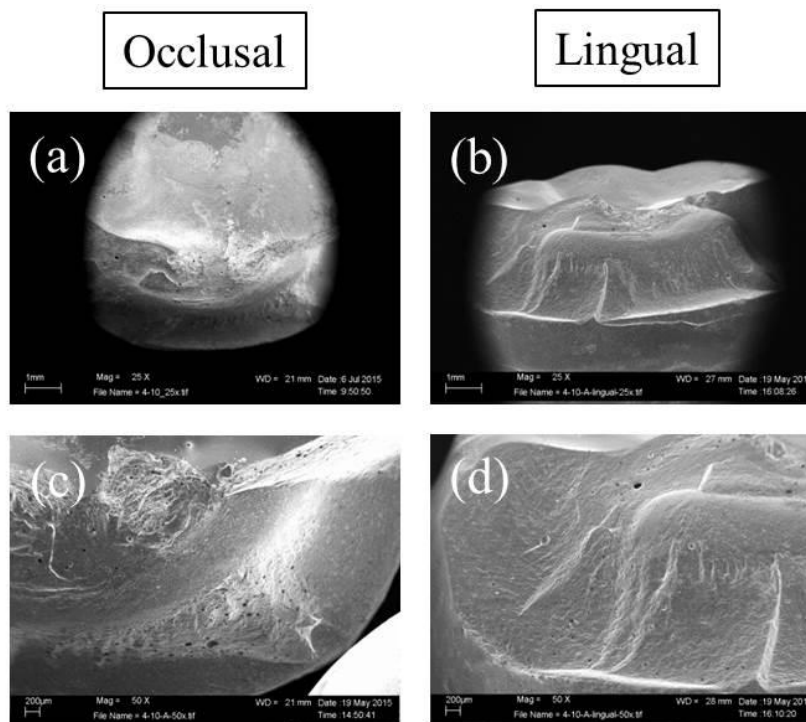


Figure 41. Scanning electron microscopy of Ce-TZP/A crown from Group 4(+). Magnification: a, b, 25 \times ; c, d, 50 \times .

Regarding chipping of porcelain veneer, the fractures originated at load-bearing points and areas (Figure 42). Crack propagations reached the lingual cervical finish line in frameworks without lingual supporting structures such as Groups 1 and 3 (Figure 43 a), or the interface of the lingual supporting structure in Groups 2 and 4 (Figure 43 b).

Stereomicroscopy and SEM revealed hackles (Figure 42, white arrows); wake hackles (Figure 42, black arrows); and arrest lines (Figure 42, black dotted arrows), indicating the direction of crack propagation towards the cervical margin and proximal area. The lingual side of Ce-TZP/A framework was exposed in more than half of specimens in each experimental group (Figure 42 a, b). In Group 4, the crack ratio on the buccal supporting structure was increased (Figure 44, black arrows).

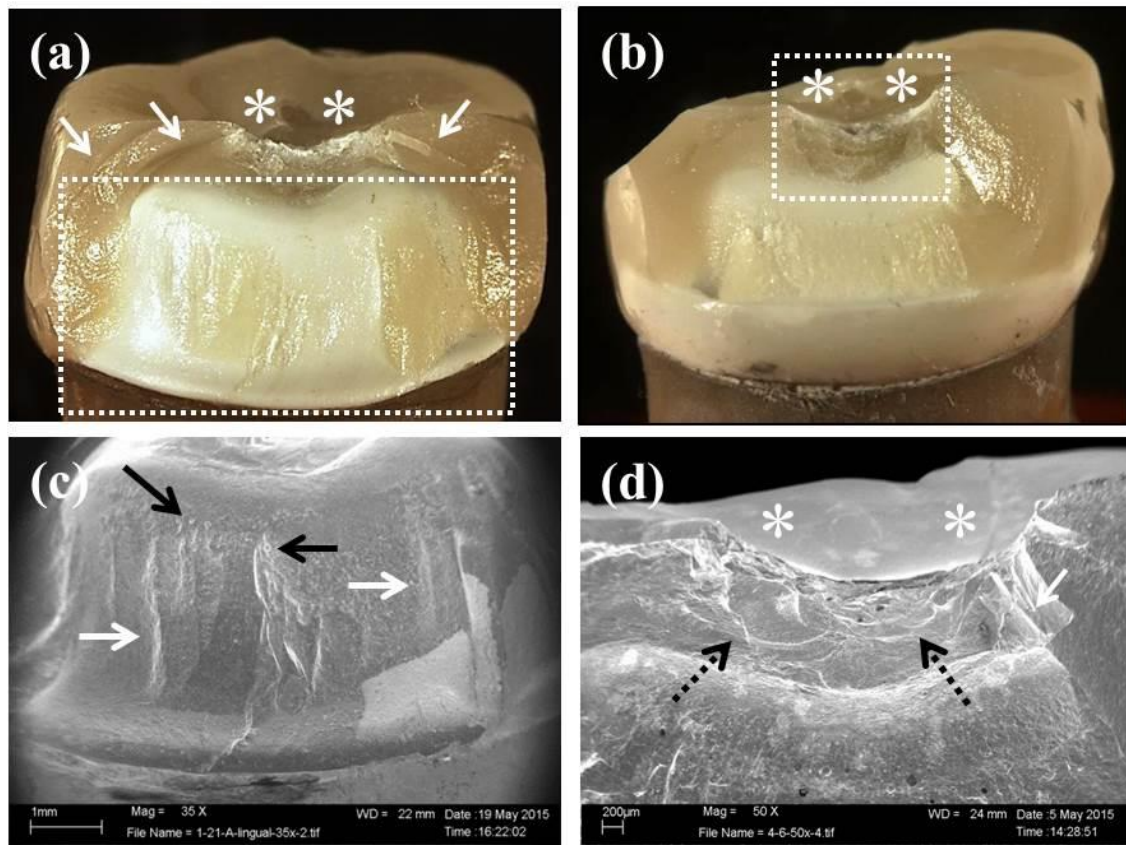


Figure 42. Stereomicroscopy (overview; a, d) and scanning electron microscopy (detail; b, c) observations of chipping of porcelain veneer. Asterisks, white arrows, black arrows, and black dotted arrows show load-bearing points, hackles, wake hackles, and arrest lines, respectively.

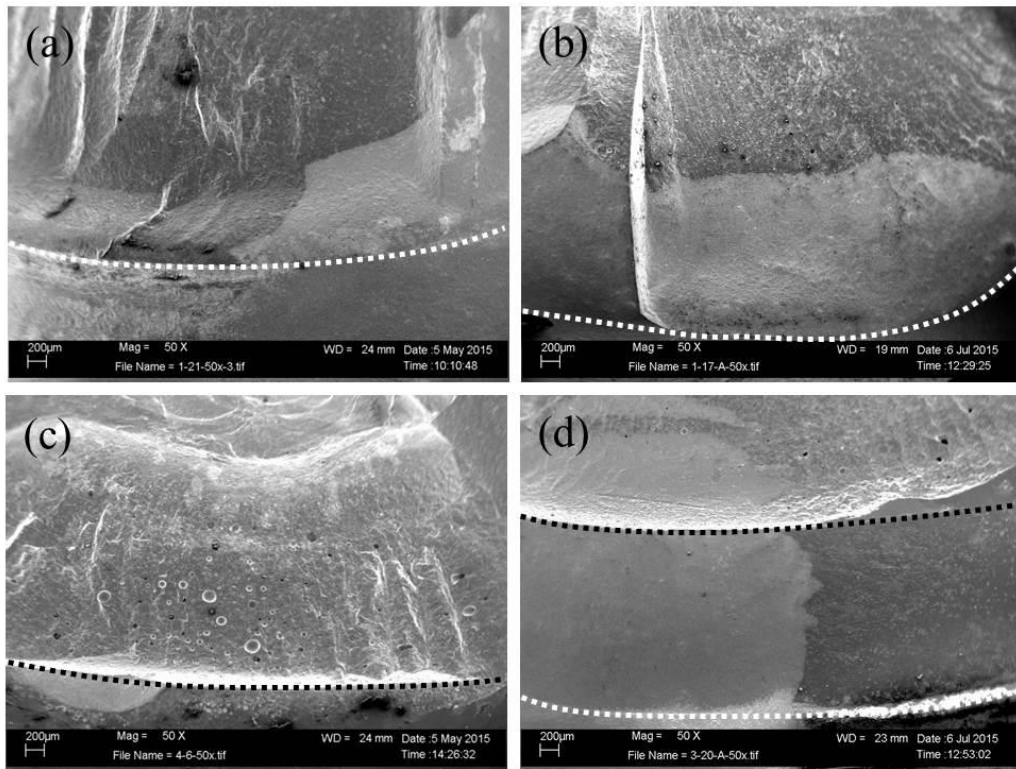


Figure 43. Scanning electron microscopy comparison of failure progression: (a, b) non-lingual supporting structure; (c, d) lingual supporting structure (50× magnification). White and black dotted lines indicate the lingual cervical margin and interface of the lingual supporting structure, respectively.

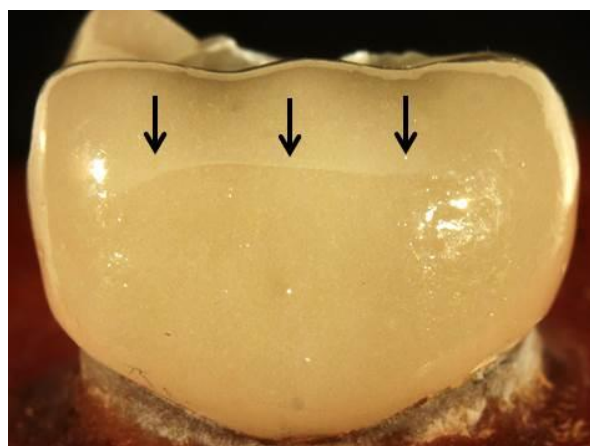


Figure 44. Stereomicroscopy observation of chipping of porcelain veneer (buccal side aspect) in Group 4. Black arrows indicate cracks.

3.3.2 Failure mode ratio

The failure mode ratio in each experimental group is given in Figure 45. Partial fracture was the most common failure mode in Groups 1–4 without mechanical preloading. The partial fracture mode ratio was 100% in Groups 1(-), 3(-), and 4(-), while the complete fracture mode ratio was 16.7% in Group 2(-). No significant difference was found among groups not subjected to mechanical preloading.

The complete fracture ratios were 16.7–41.7% in Groups 1–3 after mechanical preloading. Failure mode shifted from partial to complete fracture, and complete fracture of Group 1(+) was significantly higher than that of Group 1(-) ($p = 0.0372$). However, for Group 4(+), the partial fracture ratio still remained at 100% and complete fracture was significantly lower ($p = 0.0395$).

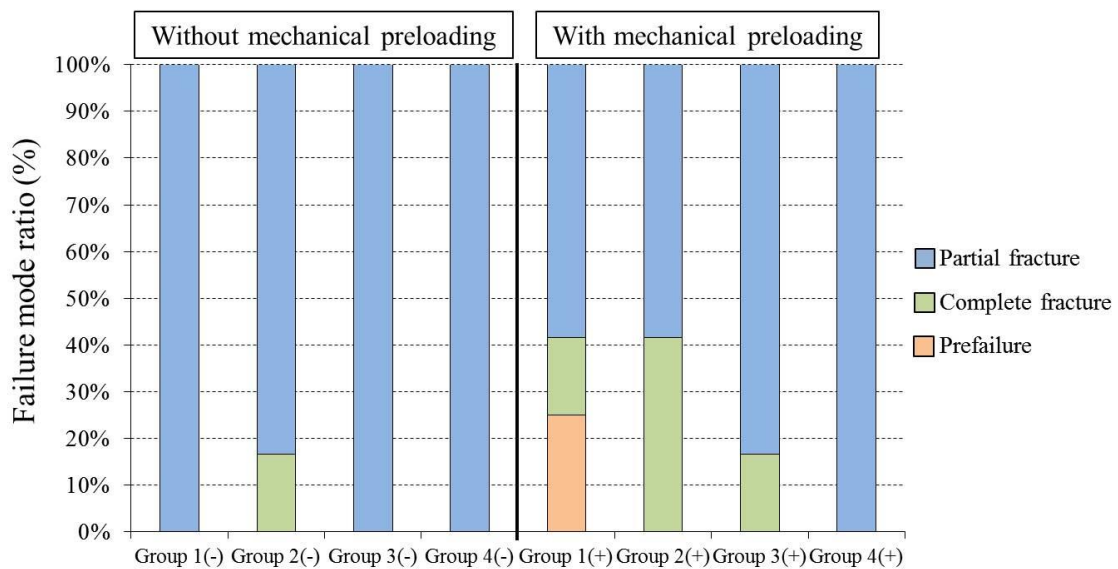


Figure 45. Failure mode ratios after mechanical preloading. Prefailure, partial fracture (cracking or chipping of porcelain veneer), and complete fracture (fracture of Ce-TZP/A framework or tooth analog).

4.0 Discussion

The focus of the present study was to evaluate the framework design of Ce-TZP/A–based all-ceramic crowns. The study was designed to investigate whether all-ceramic crowns using a novel Ce-TZP/A framework design featuring an anatomical shape with additional two-sided (buccal and lingual) supporting structures (Group 4) did not significantly differ from that of conventional anatomical framework (Group 1) or from those with an additional one-sided (buccal or lingual) supporting structure (Groups 2 and 3) in fracture load results, irrespective mechanical preloading. Failure modes were found to progress in all groups after mechanical preloading; however, this novel framework design (Group 4) inhibited failure progression. Thus, the first null hypothesis was accepted, and the second was rejected.

4.1 Framework design

The concept of a framework with additional buccal and lingual supporting structures was based on some previous studies. Modification of conventional zirconia-based crown frameworks was essential to prevent technical complications such as chipping of porcelain veneer in all-ceramic restorations. Veneering porcelain is a brittle material and requires a zirconia framework support. Chipping was known to commonly occur on the cusp or marginal ridge area of molar all-ceramic crowns. Framework designs including an anatomical shape adjusted with an even thickness of veneering porcelain showed high survival rates during 5 years of clinical observation: 94.3% among 1192 single crowns (Monaco et al. 2013), and 94.7% among 137 FPDs (Monaco et al. 2015).

Moreover, an additional lingual supporting structure created by proximally extending the lingual margin improves the support of veneering porcelain in the lingual cusp and marginal ridge areas. This design modification increases the strength not only of zirconia but also of glass-infiltrated alumina and metal ceramic frameworks (Bonfante et al. 2009). However, the buccal cusps did not correspond to a supporting structure; thus, chipping of buccal side was unfortunately not prevented.

In particular, the buccal cusp, which is located in the mandibular molar region, acts as a functional cusp and is subjected to concentrated occlusal forces during chewing and biting (Wang and Mehta 2013). Some researchers have proposed that the buccal cusp requires additional support to endure occlusal forces (Silva et al. 2011; Tinschert et al. 2008). However, a supporting structure similar to the lingual supporting structure described by Silva et al. (2011) would be directly visible if applied to the buccal side, and would thus not satisfy patients' esthetic demands. To study framework design, it is necessary to consider both esthetic standards and the ease of manufacturing.

An alternative framework design for metal-ceramic restorations has been reported (Haker 1984). This framework features a two-sided supporting structure designed by adding buccal and lingual cusps to the framework's external surface; it exhibits improved fracture strength relative to metal-ceramic. In this framework, the buccal supporting structure is invisible after application of veneering porcelain. Other researchers have also suggested specific framework designs (Tinschert et al. 2008;

Broseghini et al. 2014); however, these were so complicated that their fabrication was uneconomic. The buccal and lingual supporting structures described in this study were selected for the simplicity of their manufacture, and incorporated features of both framework designs in the internal buccal and external lingual supporting structures after veneering with porcelain.

4.2 Fracture load

Ce-TZP/A-based crowns exhibited high fracture load (approximately 2000 N) in all groups not subjected to mechanical preloading. There were no significant differences among the groups in fracture load, suggesting that framework design does not affect the results of vertical fracture loading tests, and thus, does not affect the mechanical properties of Ce-TZP/A. Ce-TZP/A has been shown to exhibit a fracture toughness of $18.3 \text{ MPa} \cdot \text{m}^{1/2}$ (Nawa et al. 1998), a value threefold higher than that of Y-TZP (Chevalier et al. 1999). In another study, a 0.3-mm-thick Ce-TZP/A framework with a lingual supporting structure was shown to exhibit higher fracture strength than a Y-TZP framework with a lingual supporting structure, but was similar fracture load with a 0.5-mm-thick Y-TZP anatomical framework (Omori et al. 2013). Further, in a single-load fracture test, a 0.5-mm-thick Y-TZP framework with an anatomical shape exhibited higher fracture load than that with a lingual supporting structure (Silva et al. 2011). Additionally, the fracture load of Y-TZP crowns with an anatomical shape was equal to that of metal-ceramic crowns with a non-anatomical shape (Alhasanyah et al. 2013). These observations suggest that all Ce-TZP/A framework designs examined in this study that were based on an anatomical shape exhibit sufficient fracture resistance in the absence of mechanical

preloading.

Generally, the influence of fatigue on fracture strength is investigated by mechanical loading and/or thermal cycling (Vult von Steyern et al. 2006; Baladhandayutham et al. 2015). In this study, only mechanical preloading to simulate mechanical fatigue was conducted. Ce-TZP/A exhibited complete resistance to LTD, whereas Y-TZP was susceptible to LTD caused by phase transformation. A previous study showed that Y-TZP exhibited decreased flexural strength after 10 h of aging, and underwent a tetragonal to monoclinic phase transformation, with the proportion of monoclinic phase increasing from 4% to around 15% (Siarampi et al. 2014). However, Ce-TZP/A has proven to be a durable biomaterial with no significant changes in monoclinic content or biaxial flexure strength after hydrothermal degradation (Ban et al. 2008).

Consequently, all groups subjected to mechanical preloading also exhibited high fracture load (1828–2374 N); there were no significant differences between groups, with the exception of Groups 1(+) and 2(+). After mechanical preloading, the crown fracture load of Groups 2, 3, and 4 tended to increase, whereas that of Group 1 tended to decrease. This difference may be explained by the existences of the supporting structure design and the zirconia transformation toughening. Hacker (1984) suggested that additional supporting structures could contact many parts of porcelain layer and obtain the compressive stress from porcelain in metal-ceramic crowns. In the present study, Group 1 frameworks featured no additional structures, and their fracture load was decreased by the fatigue caused by mechanical preloading. Conversely, the addition of structures such as buccal and/or lingual

supports increased fracture load in Groups 2–4. It was predictable that stronger binding could be formed between zirconia framework and porcelain during firing process in the supporting structures. Group 2(+) tended to be higher in fracture load than Group 3(+) and Group 4(+). This difference was caused by the location and size of the supporting structure. The lingual supporting structure, which was larger in size than the buccal supporting structure, could reduce the amounts of porcelain veneer because the whole of its surface was not veneered with porcelain. This influence of lingual supporting structure seemed to be effective compared with the compressive stress to the buccal supporting structure. Moreover, buccal supporting structure was likely to change the surface area of the occlusal surface against the vertical mechanical preloading force and the dispersion of the force. Thus, Group 4(+) tended to be higher fracture load than Group 3(+) and to be lower fracture load than Group 2(+).

The factor of zirconia phase transformation from the external stress also influenced the fracture load. Low temperature aging, which was one of external stress, changed the phase transformation and produced the positive and negative effects on the Y-TZP mechanical properties (Kim et al. 2009). The flexural strength was increased with the increase of the monoclinic contents up to 12% (transformation toughening); however, the flexural strength was decreased with the increase of more monoclinic contents. Vult von Steyern et al. (2006) showed that Y-TZP crowns exhibited higher fracture load after mechanical preloading. They stated that an increase in the fracture load was within the capacity of transformation toughening. Their study also suggested that thermal cycling was detrimental to the bond between the framework and veneering porcelain, and it decreased fracture load. Our results are in agreement

with their results of mechanical preloading. Supporting structures seemed to increase the capacity of transformation toughening and contributed to the fracture load after mechanical preloading. In contrast, fracture load decreased in Group 1(+), which had no additional supporting structures by the exceeded capacity from mechanical preloading stress. This was also supported in the confirmation of prefailure in Group 1(+). Although Ce-TZP/A is a more durable zirconia material than Y-TZP, further study is necessary to confirm the effect of thermal cycling on Ce-TZP/A-based all-ceramic crowns.

In a previous study, Y-TZP crowns exhibited higher fracture load in vertical load tests (approximately 2600-4000 N) (Kokubo et al. 2011). Other investigations of the fracture load of different veneering techniques have also shown high values (1900-6102 N) (Kanat-Ertürk et al. 2014). This difference in fracture loading test appears to be related to the abutment tooth material, which influences on fracture loads; for zirconia restorations, metal abutments yielded higher fracture load than did resin abutments (Wimmer et al. 2014; Yucel et al. 2012). One explanation for this observation is that the elastic modulus of metal (200 GPa) is higher than that of resin (11.8 GPa). The abutment material should have a low elastic modulus, similar to that of dentin (18.6 GPa), for fracture testing (Yucel et al. 2012); however, several researchers have investigated fracture load using a metal abutment (Omori et al. 2013; Stawarczyk et al. 2011). Conversely, Baladhandayutham et al. (2015) reported fracture load using resin abutments. To maximize the clinical relevance of our study, we used a resin abutment tooth because the elastic modulus of resin is similar to that of a natural tooth.

It is also necessary to consider fracture load methods. In this study, a vertical load was applied to simulate the mechanical loading of biting in a clinical situation. Some researchers have used not only vertical load but also lateral load to simulate chewing; fracture load was found to be reduced in the lateral fracture loading test, depending on the framework design. Fracture load in lateral fracture loading test of different Y-TZP framework designs was reduced by approximately 40%–55% (Kokubo et al. 2011). We identified a risk of fracture failure in Group 1(-) when we considered our results in light of this report, because the maximum voluntary molar biting force is approximately 800 N in 18-year-old males with normal occlusion (Varga et al. 2011). Furthermore, another researcher reported that the maximal molar bite force of student volunteers with a square face shape was 93.7 kg, equivalent to nearly 1000 N (Bonakdarchian et al. 2009). In clinical situations, the addition of supporting structures seems to produce acceptable fracture load with and without mechanical loading; however, these details are unclear and require further study.

4.3 Failure mode

Fracture load causes tensile stress in the porcelain veneer of bilayered all-ceramic crowns and show the different failure mode, which depends on the framework designs. Kirsten et al. (2014) investigated the stress distribution in Y-TZP crowns using the numerical finite element method with a terminal occlusion load case. This terminal occlusion case used nine loading areas. The maximum tensile stress was concentrated in the fissures between the mesiolingual and distobuccal cusps. The vertical applied loads acting on three contact points in our study was less loading areas compared to Kirsten et al. report. Thus, tensile stress seemed to be more

limited and focused in the central fossa. Thus, fracture originated at load-bearing points in all specimens. After that, the failure mode was most frequently partial fracture (e.g., chipping of porcelain veneer) in all experimental groups without mechanical preloading. The chipped area was mainly on the lingual side (Figure 32 a, e), and propagation of the cohesive/adhesive fracture reached the cervical margin (Figure 32 b, f). Crack propagation from central fossa toward the cervical margin and proximal area was identified with the indicators such as hackles and arrest lines by SEM observation (Figure 42).

However, continual compressive stress by mechanical preloading accelerated crack propagation and the degradation of porcelain veneer, increasing the incidence of complete fracture for all framework designs with the exception of Group 4. In particular, Group 1 crowns were susceptible to prefailure, which influences porcelain fatigue and the ratio of framework-to-porcelain thickness. Mechanical preloading and thermal cycling do not affect the phase-transformation or fracture properties of Ce-TZP/A (Bankoğlu Güngör et al. 2014). However, White et al. (1997) reported that cyclic mechanical fatigue influences porcelain strength. Other studies have suggested that an adequate thickness ratio of porcelain to Y-TZP is necessary, and that the incidence of cracking rises with increasing porcelain veneer thickness (Benetti et al. 2011; Guazzato et al. 2010). The ratio of porcelain to framework was higher than in this study than in others. This behavior seemed to imply that a 0.3-mm framework without additional supporting structures would offer insufficient support to an aged, thick porcelain layer.

The incidence of complete fracture was higher in Group 2(+) than in Group 3(+). This seemed to be dependent on the supporting structure. The lingual supporting structure was partially veneered with porcelain, whereas the whole of the buccal supporting structure was covered after veneering. This difference affected compressive stress on the porcelain. Furthermore, our observation that failure progression was inhibited in Group 4(+) is supported by Hacker (1984). The design of Group 4 was a more complicated structure than that of the other groups, and reduced the action of compressive stress on the veneering porcelain. Therefore, a novel framework design comprising additional buccal and lingual supporting structures would be more suitable for bilayered all-ceramic crowns.

Unfortunately, crack propagation reached the interface of the lingual support structure regardless of mechanical preloading. Chipping behavior involves many factors apart from framework design, including the ratio of porcelain to framework thickness (Jakubowicz-Kohen et al. 2014), veneering method (Schmitter et al. 2013), firing process (Paula et al. 2015), liner material (Yoon et al. 2014), and tooth preparation (Beuer et al. 2008). How these factors affect Ce-TZP/A remains unclear; further study is necessary to clarify the optimal conditions for the use of this novel framework design.

5.0 Conclusions

The aim of this study was to evaluate the fracture load and failure mode of all-ceramic crowns using different ceria-stabilized zirconia/alumina nanocomposite (Ce-TZP/A)-based framework designs. Within the limitations of this study, it can be concluded that:

1. The fracture load of all-ceramic crowns with a novel Ce-TZP/A framework using an anatomical shape and additional two-sided (buccal and lingual) supporting structures does not significantly differ from other groups, irrespective of mechanical preloading.
2. The most common fracture mode was chipping of porcelain veneer without mechanical preloading. Mechanical preloading promoted failure progression (from partial to complete fracture) in framework designs without additional supporting structures and with one-sided (buccal or lingual) supporting structures.
3. However, a framework with additional two-sided (buccal and lingual) supporting structures inhibited failure progression after mechanical preloading, suggesting that this is a durable framework design.

6.0 Summary

Purpose: Framework modification is essential to reduce chipping of the veneering porcelain in bilayered all-ceramic restorations. However, conventional modifications are insufficient, because buccal cusps did not correspond to a supporting structure. We manufactured a novel framework design, featuring an anatomical shape with additional two-sided (buccal and lingual) supporting structures, from ceria-stabilized tetragonal zirconia/alumina nanocomposite (Ce-TZP/A), and compared the fracture load and failure mode of all-ceramic crowns with Ce-TZP/A frameworks of different designs.

Methods: Four different Ce-TZP/A framework designs were fabricated using CAD/CAM system. The framework designs were as follow; Group 1: anatomical shape; Group 2: with an additional lingual supporting structure; Group 3: with an additional buccal supporting structure; Group 4: with additional buccal and lingual supporting structures. Each framework was veneered with feldspathic ceramic and then cemented to resin tooth analog using self-adhesive resin cement. Fracture load of each crown either without or with mechanical preloading was measured using a universal testing machine. Scanning electron microscopy and stereomicroscopy were performed to classify failure mode as either partial fracture (cracking or chipping of porcelain veneer) or complete fracture (fracture of Ce-TZP/A framework or tooth analog).

Results: Three crowns in Group 1 exhibited prefailure by mechanical preloading. Fracture load ranged from 1866–2049 N without mechanical preloading, and from 1828–2374 N with mechanical preloading; fracture load was not significant for any of the framework designs without mechanical preloading. Furthermore, fracture load did not significantly differ between framework designs except Group 1 with mechanical preloading. The most common failure mode was chipping of porcelain veneer without

mechanical preloading. Although mechanical preloading promoted failure progression (from partial to complete fracture) in Groups 1–3, failure progression was inhibited in Group 4.

Conclusion: This novel Ce-TZP/A framework design has the potential to reduce chipping of the veneering porcelain and improve zirconia based all-ceramic restoration reliability.

Keywords: Ce-TZP/A, framework design, zirconia, fracture load, failure mode

7.0 Zusammenfassung

Ziel: Um Verblendkeramikfrakturen (Chipping) bei vollkeramischen Restaurationen zu minimieren ist die anatomische Gerüststruktur ein wesentlicher Faktor der zum Langzeitverhalten einer solchen Restauration beiträgt. Jedoch sind herkömmliche Modifikationen unzureichend, weil die bukkalen Höcker bzw. die linguale Schulter nicht direkt unterstützt werden. In dieser Studie wurden deshalb die Gerüststrukturen soweit modifiziert, dass die konventionelle anatomische Gerüststruktur mit zusätzlichen Unterstützungszonen (bukkal und lingual) gefertigt wurden. Für das Gerüstmaterial wurde ein mit Cer-Oxid verstärktes Zirkoniumdioxid verwendet (Ce-TZP-A) und mit einer entsprechenden Verblendkeramik versehen. Alle Gruppen wurden hinsichtlich ihrer Frakturstabilität und Bruchmodi untersucht. Herauszufinden galt es, ob die hier beschriebenen Modifikationen einen positiven Effekt auf die Frakturstabilität haben.

Methoden: Vier verschiedene Gerüststrukturen aus Ce-TZP-A wurden mittels CAD/CAM Fertigung hergestellt: Gruppe 1: anatomische Form; Gruppe 2: mit zusätzlicher lingualen Schulterunterstützung; Gruppe 3: mit zusätzlicher bukkalen

Höckerunterstützung; Gruppe 4: mit zusätzlicher bukkalen Höckerunterstützung und lingualer Schulterunterstützung. Jede Gruppe wurde mit einer Feldspatkeramik verblendet und auf einem Kunststoff-Stumpf zementiert. Um die Proben mechanisch zu altern wurde ein Kausimulator verwendet und somit eine Tragedauer von ca. 5 Jahren simuliert. Frakturstabilität für jede Probe wurde mittels einer Universalprüfmaschine ermittelt (Bruchlast in Newton). Nach der Prüfung wurden die Proben mittels eines Stereomikroskops und Rasterelektronen-Mikroskops untersucht und nach verschiedenen Bruchmodi eingeteilt: teilweise Fraktur (Risse oder Chipping); komplette Fraktur (Bruch des Gerüsts oder Kunststoff-Stumpf).

Ergebnisse: Nach der mechanischen Alterung fielen drei Kronen aus Gruppe 1 wegen totalem Versagen aus. Die Bruchlast der Gruppen ohne mechanische Alterung lag im Bereich von 1866-2049 N und für die Gruppen mit mechanischer Alterung zwischen 1828-2374 N. Mit Ausnahme von Gruppe 1 unterschied sich die Frakturstabilität in den Gruppen mit und ohne mechanische Alterung nicht signifikant voneinander. Die am meisten beobachtete Fehlerform war Chipping der Verblendkeramik in den Gruppen ohne mechanische Alterung. Währenddessen die Gruppen 1-3 mit mechanischer Alterung ein gemischtes Fehlerverhalten zeigten. Gruppe 4 zeigte hier nur teilweise Frakturen der Verblendkeramik.

Fazit: Die in dieser Studie vorgestellte Modifizierung von aus Ce-TZP-A hergestellten Gerüsten, stellt eine mögliche Alternative für vollkeramische Restaurationen dar um eventuelle Komplikationen zu vermindern und die Zuverlässigkeit zu erhöhen.

Stichworte: Ce-TZP/A, Gerüst-Design, Zirkoniumdioxid, Bruchfestigkeit, Bruchmodus

8.0 Author contribution

Tomofumi Sawada conceived, designed, and performed the experiments. Tomofumi Sawada also analyzed the data.

Mr. Sebastian Spintzyk, Scientific staff of the Section Medical Materials Science and Technology, Dental Faculty, Eberhard Karls University Tübingen, advised and contributed to the preparing of the specimens.

ZTM Ekkehard Kröwerath, Cheif of the Dental laboratory, University Hospital Tübingen, advised and contributed to the preparing of the specimens.

Ms. Christine Schille, Technical assistant of the Section Medical Materials Science and Technology, Dental Faculty, Eberhard Karls University Tübingen, performed and contributed to the experiments of fracture loading test.

Mr. Ernst Schweizer, Technical assistant of the Section Medical Materials Science and Technology, Dental Faculty, Eberhard Karls University Tübingen, performed and contributed to the experiments of scanning electron microscopy.

Prof. Dr. Jürgen Geis-Gerstorfer, Director of the Section Medical Materials Science and Technology, Dental Faculty, Eberhard Karls University Tübingen, commented the research work.

9.0 References

- Aldegheishem A, Alfaer A, Brezavšček M, Vach K, Eliades G, Att W. 2015. Wear behavior of zirconia substrates against different antagonist materials. *Int J Esthet Dent*. 10(3):468-485.
- Alhasanyah A, Vaidyanathan TK, Flinton RJ. 2013. Effect of core thickness differences on post-fatigue indentation fracture resistance of veneered zirconia crowns. *J Prosthodont*. 22(5):383-290.
- Andersson M, Odén A. 1993. A new all-ceramic crown. A dense-sintered, high-purity alumina coping with porcelain. *Acta Odontol Scand*. 51(1):59-64.
- Agustín-Panadero R, Román-Rodríguez JL, Ferreiroa A, Solá-Ruíz MF, Fons-Font A. 2014. Zirconia in fixed prosthesis. A literature review. *J Clin Exp Dent*. 6(1):e66-73.
- Baladhandayutham B, Lawson NC, Burgess JO. 2015. Fracture load of ceramic restorations after fatigue loading. *Prosthet Dent*. 114(2):266-271.
- Ban S, Sato H, Suehiro Y, Nakanishi H, Nawa M. 2008. Biaxial flexure strength and low temperature degradation of Ce-TZP/Al₂O₃ nanocomposite and Y-TZP as dental restoratives. *J Biomed Mater Res Part B: Appl Biomater*. 87(2):492-498.
- Bankoğlu Güngör M, Yılmaz H, Aydın C, Karakoca Nemli S, Turhan Bal B, Tıraş T. 2014. Biaxial flexural strength and phase transformation of Ce-TZP/Al₂O₃ and Y-TZP core materials after thermocycling and mechanical loading. *J Adv Prosthodont*. 6(3):224-232.
- Benetti P, Pelogia F, Valandro LF, Bottino MA, Bona AD. 2011. The effect of porcelain thickness and surface liner application on the fracture behavior of a ceramic system. *Dent Mater*. 27(9):948-953.
- Beuer F, Aggstaller H, Edelhoff D, Gernet W. 2008. Effect of preparation design on the fracture resistance of zirconia crown copings. *Dent Mater J*. 27(3):362-367.
- Beuer F, Stimmelmayer M, Gernet W, Edelhoff D, Güh JF, Naumann M. 2010. Prospective study of zirconia-based restorations: 3-year clinical results. *Quintessence Int*. 41(8):631-637.
- Blaise L, Villermaux F, Cales B. 2001. Ageing of zirconia: everything you always wanted to know. *Key Engineering Materials*. 192: 553-556.
- Boitelle P, Mawussi B, Tapie L, Fromentin O. 2014. A systematic review of CAD/CAM fit restoration evaluations. *J Oral Rehabil*. 41(11):853-874.
- Bonakdarchian M, Askari N, Askari M. 2009. Effect of face form on maximal molar

- bite force with natural dentition. *Arch Oral Biol.* 54(3):201-204.
- Bonfante EA, Rafferty B, Zavanelli RA, Silva NR, Rekow ED, Thompson VP, Coelho PG. 2010. Thermal/mechanical simulation and laboratory fatigue testing of an alternative yttria tetragonal zirconia polycrystal core-veneer all-ceramic layered crown design. *Eur J Oral Sci.* 118(2):202-209.
- Bonfante EA, da Silva NRFA, Coelho PG, Bayardo-Gonzalez, Thompson VP, Bonfante G. 2009. Effect of framework design on crown failure. *Eur J Oral Sci.* 117(2):194-199.
- Broseghini C, Broseghini M, Gracis S, Vigolo P. 2014. Aesthetic functional area protection concept for prevention of ceramic chipping with zirconia frameworks. *Int J Prosthodont.* 27(2):174-176.
- Cattani-Lorente M, Scherrer SS, Ammann P, Jobin M, Wiskott HW. 2011. Low temperature degradation of a Y-TZP dental ceramic. *Acta Biomater.* 7(2):858-865.
- Cales B. 2000. Zirconia as a sliding material: histologic, laboratory, and clinical data. *Clin Orthop Relat Res.* 379:94-112.
- Chevalier J, Olganon C, Fantozzi G. 1999. Subcritical crack propagation in 3 Y-TZP ceramics. *J Am Cerac Soc.* 82(11):3129-3138.
- Chevalier J. 2006. What future for zirconia as a biomaterial? *Biomaterials.* 27(4):535-543.
- Christel P, Meunier A, Dorlot JM, Crolet JM, Witvoet J, Sedel L, Boutin P. 1988. Biomechanical compatibility and design of ceramic implants for orthopedic surgery. *Ann N Y Acad Sci.* 523:234-56.
- Clarke IC, Manaka M, Green DD, Williams P, Pezzotti G, Kim YH, Ries M, Sugano N, Sedel L, Delauney C, Nissan BB, Donaldson T, Gustafson GA. 2003. Current status of zirconia used in total hip implants. *J Bone Joint Surg Am.* 85A Suppl 4:73-84.
- Denry I, Kelly JR. 2008. State of the art of zirconia for dental applications. *Dent Mater.* 24(3):299-307, 2008.
- Donovan TE. 2008. Factors essential for successful all-ceramic restorations. *J Am Dent Assoc.* 139(Suppl):14S-18S.
- Duret F, Preston JD. 1991. CAD/CAM imaging in dentistry. *Curr Opin Dent.* 1:150-154.
- Ferrari M, Giovannetti A, Carrabba M, Bonadeo G, Rengo C, Monticelli F, Vichi A. 2014. Fracture resistance of three porcelain-layered CAD/CAM zirconia frame designs. *Dent Mater.* 30(7):e163-168.

- Gracis S, Thompson VP, Ferencz JL, Silva NR, Bonfante EA. 2015. A new classification system for all-ceramic and ceramic-like restorative materials. *Int J Prosthodont.* 28(3):227-235.
- Guazzato M, Proos K, Quach L, Swain MV. 2004. Strength, reliability and mode of fracture of bilayered porcelain/zirconia (Y-TZP) dental ceramics. *Biomaterials.* 25(20):5045-5052.
- Guazzato M, Walton TR, Franklin W, Davis G, Bohl C, Klineberg I. 2010. Influence of thickness and cooling rate on development of spontaneous cracks in porcelain/zirconia structures. *Aust Dent J.* 55(3):306-310.
- Guess PC, Bonfante EA, Silva NR, Coelho PG, Thompson VP. 2013. Effect of core design and veneering technique on damage and reliability of Y-TZP-supported crowns. *Dent Mater.* 29(3):307-316.
- Ha SR, Kim SH, Han JS, Yoo SH, Jeong SC, Lee JB, Yeo IS. 2013. The influence of various core designs on stress distribution in the veneered zirconia crown: a finite element analysis study. *J Adv Prosthodont.* 5(2):187-197.
- Haker G. 1984. Structural design for a metal framework (I). *Quintessenz Zahntech.* 10(1):83-91.
- Hannink RHJ, Kelly PM, Muddle BC. 2000. Transformation toughening in zirconia-containing ceramics. *J Am Ceram Soc.* 83:461-487.
- Heintze SD, Rousson V. 2010. Survival of zirconia- and metal-supported fixed dental prostheses: a systematic review. *Int J Prosthodont.* 23(6):493-502.
- Jakubowicz-Kohen BD, Sadoun MJ, Douillard T, Mainjot AK. 2014. Influence of firing time and framework thickness on veneered Y-TZP discs curvature. *Dent Mater.* 30(2):242-248.
- Kanat-Ertürk B, Cömlekoğlu EM, Dündar-Çömlekoğlu M, Ozcan M, Güngör MA. 2014. Effect of veneering methods on zirconia framework-veneer ceramic adhesion and fracture resistance of single crowns. *J Prosthodont.* Available from URL: <http://www.ncbi.nlm.nih.gov/pubmed/25319017>(doi: 10.1111/jopr.12236.)
- Karimipour-Saryazdi M, Sadid-Zadeh R, Givan D, Burgess JO, Ramp LC, Liu PR. 2010. Influence of surface treatment of yttrium-stabilized tetragonal zirconium oxides and cement type on crown retention after artificial aging. *J Prosthet Dent.* 111(5):395-403.
- Kim HT, Han JS, Yang JH, Lee JB, Kim SH. 2009. The effect of low temperature aging on the mechanical property & phase stability of Y-TZP ceramics. *J Adv Prosthodont.* 1(3):113-117.

- Kirsten A, Parkot D, Raith S, Fischer H. 2014. A cusp supporting framework design can decrease critical stresses in veneered molar crowns. *Dent Mater.* 30(3):321-326.
- Kokubo Y, Tsumita M, Kano T, Fukushima S. 2011. The influence of zirconia coping designs on the fracture load of all-ceramic molar crowns. *Dent Mater J.* 30(3):281-285.
- Kolbeck C, Rosentritt M, Lang R, Handel G. 2006. Discoloration of facing and restorative composites by UV-irradiation and staining food. *Dent Mater.* 22(1):63-68.
- Li RW, Chow TW, Matinlinna JP. 2014. Ceramic dental biomaterials and CAD/CAM technology: state of the art. *J Prosthodont Res.* 58(4):208-16.
- Larsson C, Wennerberg A. 2014. The clinical success of zirconia-based crowns: a systematic review. *Int J Prosthodont.* 27(1):33-43.
- Lorenzoni FC, Martins LM, Silva NR, Coelho PG, Guess PC, Bonfante EA, Thompson VP, Bonfante G. 2010. Fatigue life and failure modes of crowns systems with a modified framework design. *J Dent.* 38(8):626-634.
- Marchack BW, Futatsuki Y, Marchack CB, White SN. 2008. Customization of milled zirconia copings for all-ceramic crowns: A clinical report. *J Prosthet Dent.* 99(3):169-173.
- Miragaya L, Maia LC, Sabrosa CE, de Goes MF, da Silva EM. 2011. Evaluation of self-adhesive resin cement bond strength to yttria-stabilized zirconia ceramic (Y-TZP) using four surface treatments. *J Adhes Dent.* 13(5):473-480.
- Miyazaki T, Hotta Y. 2011. CAD/CAM systems available for the fabrication of crown and bridge restorations. *Aust Dent J.* 56:97-106.
- Miyazaki T, Hotta Y, Kunii J, Kuriyama S, Tamaki Y. 2009. A review of dental CAD/CAM: current status and future perspectives from 20 years of experience. *Dent Mater J.* 28(1):44-56.
- Miyazaki T, Nakamura T, Matsumura H, Ban S, Kobayashi T. 2013. Current status of zirconia restoration. *J Prosthodont Res.* 57(4):236-261.
- Monaco C, Caldari M, Scotti R. 2013. Clinical evaluation of 1,132 zirconia-based single crowns: a retrospective cohort study from the AIOP clinical research group. *Int J Prosthodont.* 26(5):435-442.
- Monaco C, Caldari M, Scotti R. 2015. Clinical evaluation of tooth-supported zirconia-based fixed dental prostheses: a retrospective cohort study from the AIOP clinical research group. *Int J Prosthodont.* 28(3):236-238.
- Mörmann WH, Brandestini M, Lutz F, Barbakow F. 1989. Chairside computer-aided

- direct ceramic inlays. *Quintessence Int.* 20(5):329-339.
- Nawa M, Nakamoto S, Sekino T, Niihara K. 1998. Tough and strong Ce-TZP/Alumina nanocomposites doped with titania. *Ceram Int.* 24(7):497-506.
- Okabayashi S, Nomoto S, Sato T, Miho O. 2013. Influence of proximal supportive design of zirconia framework on fracture load of veneering porcelain. *Dent Mater J.* 32(4):572-577.
- Omata Y, Uno S, Nakaoki Y, Tanaka T, Sano H, Yoshida S, Sidhu SK. 2006. Staining of hybrid composites with coffee, oolong tea, or red wine. *Dent Mater J.* 25(1):125-131.
- Omori S, Komada W, Yoshida K, Miura H. 2013. Effect of thickness of zirconia-ceramic crown frameworks on strength and fracture pattern. *Dent Mater J.* 32(1):189-194.
- Paula VG, Lorenzoni FC, Bonfante EA, Silva NR, Thompson VP, Bonfante G. 2015. Slow cooling protocol improves fatigue life of zirconia crowns. *Dent Mater.* 31(2):77-87.
- Pelaez J, Cogolludo PG, Serrano B, Serrano JF, Suarez MJ. 2012. A four-year prospective clinical evaluation of zirconia and metal-ceramic posterior fixed dental prostheses. *Int J Prosthodont* 25(5):451-458.
- Pereira Lde L, Campos F, Dal Piva AM, Gondim LD, Souza RO, Özcan M. 2015. Can application of universal primers alone be a substitute for airborne-particle abrasion to improve adhesion of resin cement to zirconia? *J Adhes Dent.* 17(2):169-174.
- Pjetursson BE, Sailer I, Makarov NA, Zwahlen M, Thoma DS. 2015. All-ceramic or metal-ceramic tooth-supported fixed dental prostheses (FDPs)? A systematic review of the survival and complication rates. Part II: Multiple-unit FDPs. *Dent Mater.* 31(6):624-639.
- Pjetursson BE, Sailer I, Zwahlen M, Hämmerle CH. 2007. A systematic review of the survival and complication rates of all-ceramic and metal-ceramic reconstructions after an observation period of at least 3 years. Part I: Single crowns. *Clin Oral Implants Res.* 18(Suppl 3):73-85.
- Philipp A, Fischer J, Hämmerle CH, Sailer I. 2010. Novel ceria-stabilized tetragonal zirconia/alumina nanocomposite as framework material for posterior fixed dental prostheses: preliminary results of a prospective case series at 1 year of function. *Quintessence Int.* 41(4):313-319.
- Rekow ED. 1991. Dental CAD-CAM Systems: What Is the State of the Art? *J Am*

- Dent Assoc 122(12):43-48.
- Roediger M, Gersdorff N, Huels A, Rinke S. 2010. Prospective evaluation of zirconia posterior fixed partial dentures: four-year clinical results. *Int J Prosthodont.* 23(2):141-148.
- Rosentritt M, Steiger D, Behr M, Handel G, Kolbeck C. 2009. Influence of substructure design and spacer settings on the in vitro performance of molar zirconia crowns. *J Dent.* 37(12):978-983.
- Rossetti PH, do Valle AL, de Carvalho RM, De Goes MF, Pegoraro LF. 2008. Correlation between margin fit and microleakage in complete crowns cemented with three luting agents. *J Appl Oral Sci.* 16(1):64-69.
- Sailer I, Fehér A, Filser F, Lüthy H, Gauckler LJ, Schärer P, Franz Hämmerle CH. 2006. Prospective clinical study of zirconia posterior fixed partial dentures: 3-year follow-up. *Quintessence Int.* 37(9):685-693.
- Sailer I, Makarov NA, Thoma DS, Zwahlen M, Pjetursson BE. 2015. All-ceramic or metal-ceramic tooth-supported fixed dental prostheses (FDPs)? A systematic review of the survival and complication rates. Part I: Single crowns (SCs). *Dent Mater.* 31(6):603-623.
- Schley JS, Heussen N, Reich S, Fischer J, Haselhuhn K, Wolfart S. 2010. Survival probability of zirconia-based fixed dental prostheses up to 5 yr: a systematic review of the literature. *Eur J Oral Sci.* 118(5):443-450.
- Schmitter M, Mueller D, Rues S. 2013. In vitro chipping behaviour of all-ceramic crowns with a zirconia framework and feldspathic veneering: comparison of CAD/CAM-produced veneer with manually layered veneer. *J Oral Rehabil.* 40(7):519-525.
- Shimizu K, Oka M, Kumar P, Kotoura Y, Yamamuro T, Makinouchi K, Nakamura T. 1993. Time-dependent changes in the mechanical properties of zirconia ceramic. *J Biomed Mater Res.* 27(6):729-734.
- Siarampi E, Kontonasaki E, Andrikopoulos KS, Kantiranis N, Voyiatzis GA, Zorba T, Paraskevopoulos KM, Koidis P. 2014. Effect of in vitro aging on the flexural strength and probability to fracture of Y-TZP zirconia ceramics for all-ceramic restorations. *Dent Mater.* 30(12):e306-316.
- Silva NR, Bonfante EA, Rafferty BT, Zavanelli RA, Rekow ED, Thompson VP, Coelho PG. 2011. Modified Y-TZP core design improves all-ceramic crown reliability. *J Dent Res.* 90(1):104-108.
- Stawarczyk B, Ozcan M, Roos M, Trottmann A, Hämmerle CH. 2011. Fracture load and failure analysis of zirconia single crowns veneered with pressed and

- layered ceramics after chewing simulation. *Dent Mater J.* 30(4):554-562.
- Tanaka K, Tamura J, Kawanabe K, Nawa M, Uchida M, Kokubo T, Nakamura T. 2003. Phase stability after aging and its influence on pin-on-disk wear properties of Ce-TZP/Al₂O₃ nanocomposite and conventional Y-TZP. *J Biomed Mater Res A.* 67(1):200-207.
- Tanaka S, Takaba M, Ishiura Y, Kamimura E, Baba K. 2015. A 3-year follow-up of ceria-stabilized zirconia/alumina nanocomposite (Ce-TZP/A) frameworks for fixed dental prostheses. *J Prosthodont Res.* 59(1):55-61.
- Tinschert J, Schulze KA, Natt G, Latzke P, Heussen N, Spiekermann H. 2008. Clinical behavior of zirconia-based fixed partial dentures made of DC-Zirkon: 3-year results. *Int J Prosthodont.* 21(3):217-222.
- Thompson VP, Rekow DE. 2004. Dental ceramics and the molar crown testing ground. *J Appl Oral Sci.* 12(spe):26-36.
- Tsukima K, Shimada M. 1985. Strength, fracture toughness and Vickers hardness of CeO₂-stabilized tetragonal ZrO₂ polycrystals (Ce-TZP). *J Mater Sci.* 20:1178-1184.
- Tuncdemir AR, Aykent F. 2012. Effects of fibers on the color change and stability of resin composites after accelerated aging. *Dent Mater J.* 31(5):872-878.
- Varga S, Spalj S, Lapter Varga M, Anic Milosevic S, Mestrovic S, Slaj M. 2011. Maximum voluntary molar bite force in subjects with normal occlusion. *Eur J Orthod.* 33(4):427-433.
- Vult von Steyern P, Ebbesson S, Holmgren J, Haag P, Nilner K. 2006. Fracture strength of two oxide ceramic crown systems after cyclic pre-loading and thermocycling. *J Oral Rehabil.* 33(9):682-689.
- Wang M, Mehta N. 2013. A possible biomechanical role of occlusal cusp-fossa contact relationships. *J Oral Rehabil.* 40(1):69-79.
- Wassermann A, Kaiser M, Strub JR. 2006. Clinical long-term results of VITA In-Ceram Classic crowns and fixed partial dentures: A systematic literature review. *Int J Prosthodont.* 19(4):355-363.
- White SN, Li ZC, Yu Z, Kipnis V. 1997. Relationship between static chemical and cyclic mechanical fatigue in a feldspathic porcelain. *Dent Mater.* 13(2):103-110.
- Wimmer T, Erdelt KJ, Eichberger M, Roos M, Edelhoff D, Stawarczyk B. 2014. Influence of abutment model materials on the fracture loads of three-unit fixed dental prostheses. *Dent Mater J.* 33(6):717-724.
- Wittneben JG, Wright RF, Weber HP, Gallucci GO. 2009. A systematic review of the

- clinical performance of CAD/CAM single-tooth restorations. *Int J Prosthodont.* 22(5):466-471.
- Yoon HI, Yeo IS, Yi YJ, Kim SH, Lee JB, Han JS. 2014. Effect of surface treatment and liner material on the adhesion between veneering ceramic and zirconia. *J Mech Behav Biomed Mater.* 40:369-374.
- Yoshimura M, Noma T, Kawabata K, Somiya S. 1987. Role of H₂O on the degradation process of Y-TZP. *J Mater Sci Lett.* 6:465-467.
- Yucel MT, Yondem I, Aykent F, Eraslan O. 2012. Influence of the supporting die structures on the fracture strength of all-ceramic materials. *Clin Oral Investig.* 16(4):1105-1110.

10.0 Appendix

10.1 Microscopy and SEM of prefailure in Ce-TZP/A crown after mechanical preloading

After mechanical preloading, prefailures were found in Group 1(+). One specimen of prefailure including chipping of porcelain veneer was observed with stereomicroscopy (Figure 46 a, b) and SEM (Figure 46 c–f).

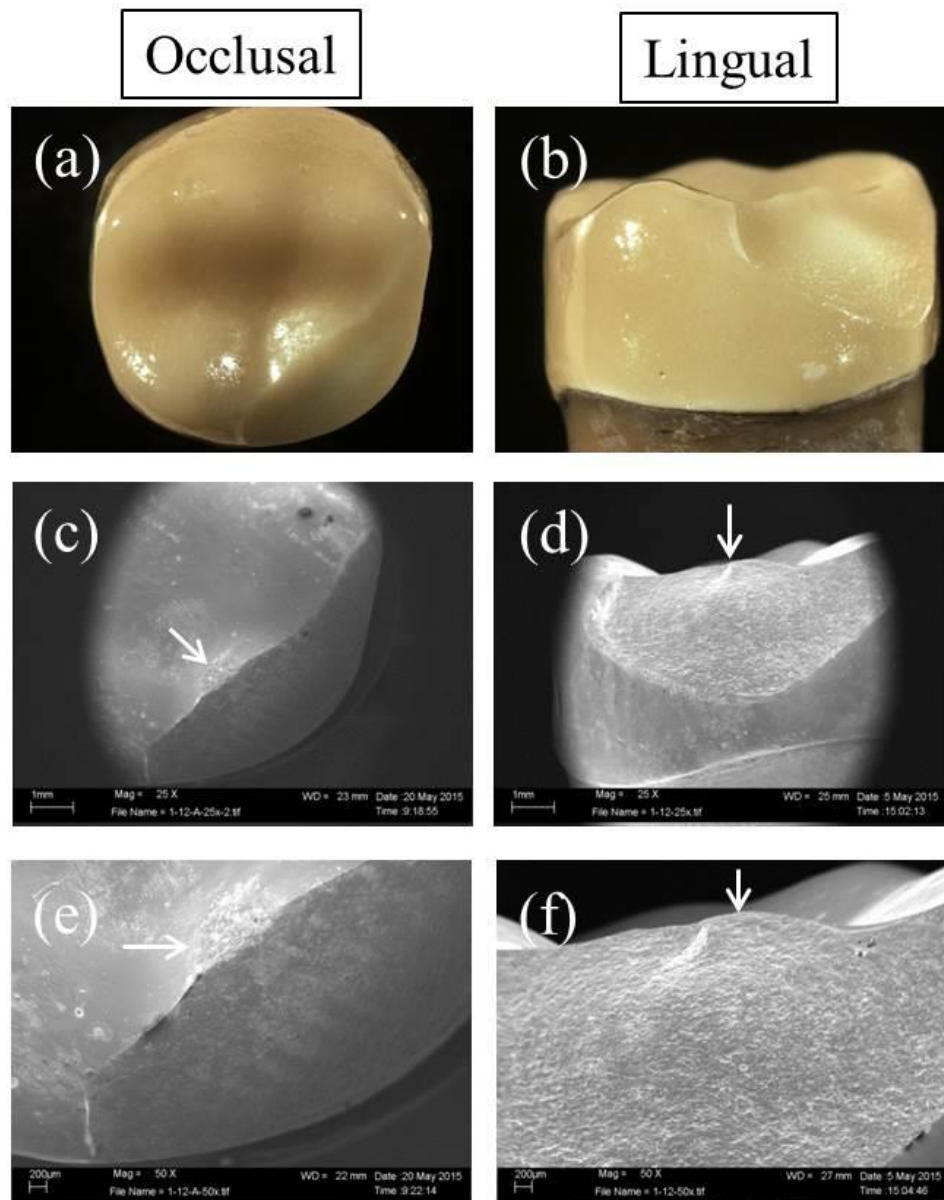


Figure 46. Stereomicroscopy (a, b) and scanning electron microscopy (c–f) of Ce-TZP/A crown from Group 1(+) with prefailure after mechanical preloading. White arrows indicate the starting point of the fracture (c–f). Magnification: a, 7 \times ; b, 8 \times ; c, d, 25 \times ; e, f, 50 \times .)

10.2 Details of distribution of failure modes in Ce-TZP/A crowns with different framework designs

The percentage of failure modes in each experimental group is given in Table 10. In Groups 1–3, the percentages of complete fracture compared to partial fracture were increased after mechanical preloading. The percentage of partial fracture in Group 4 was not changed after mechanical preloading.

The failure mode was shifted from partial to complete fracture in Groups 1–3, indicating failure progression after mechanical preloading. However, failure progression was prevented in Group 4.

Table 10. Distribution of failure modes in Ce-TZP/A crowns with different framework designs.

Experimental group	Failure mode (%)		
	Partial fracture	Complete fracture	Prefailure
Group 1(-)	100	0	0
Group 1(+)	58.3	16.7	25.0
Group 2(-)	83.3	16.7	0
Group 2(+)	58.3	41.7	0
Group 3(-)	100	0	0
Group 3(+)	83.3	16.7	0
Group 4(-)	100	0	0
Group 4(+)	100	0	0

Prefailure, chipping of porcelain veneer after mechanical preloading; partial fracture, cracking or chipping of porcelain veneer; complete fracture, fracture of Ce-TZP/A framework or tooth analog. Group 1, occlusal anatomical shape; Group 2, with additional lingual supporting structure; Group 3, with additional buccal supporting structure; Group 4, with additional lingual and buccal supporting structures.

10.3 Analysis of fracture loads in different failure modes

The fracture loads in different failure modes are given in Figures 47 and 48. Fracture loads ranged from 1756 ± 336 N (cracking of porcelain veneer) to 2384 ± 329 N (fracture of tooth analog) (Figure 47). The fracture load in fracture of tooth analog was significantly higher than that in cracking or chipping of porcelain veneer ($p < 0.05$ and 0.01 , respectively). The fracture load in complete fracture (2342 ± 322 N) was significantly higher than that in partial fracture (1981 ± 422 N, $p < 0.01$) (Figure 48).

Analysis of fracture load by failure mode revealed that with increasing fracture load, the failure mode progressed from partial to complete fracture.

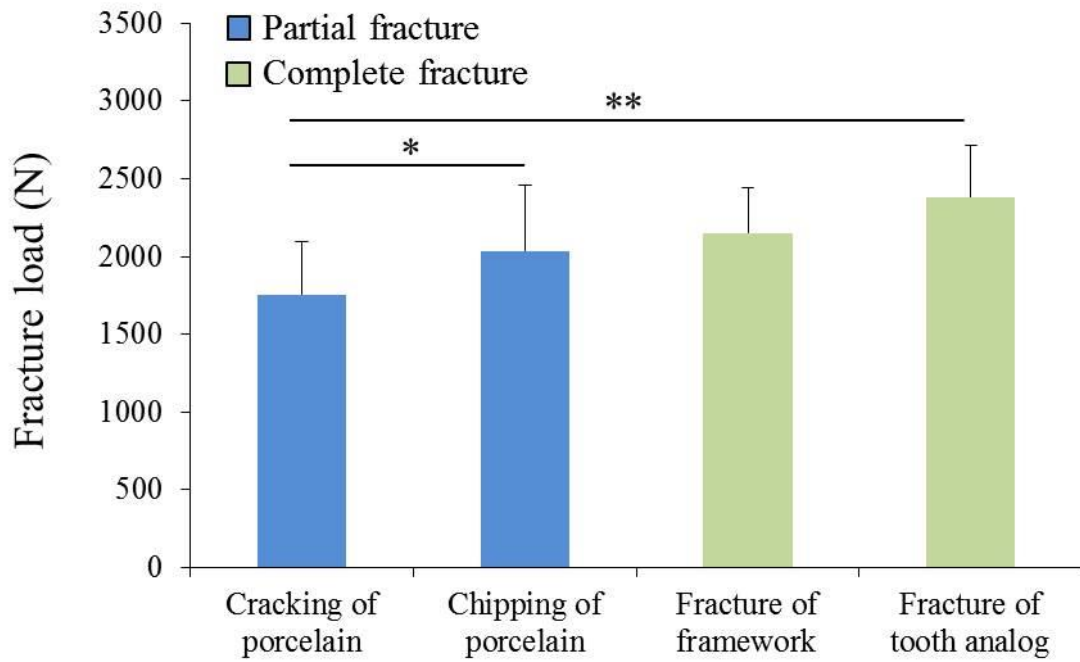


Figure 47. Fracture load in each failure mode. Results were analyzed with a 1-way analysis of variance and a post hoc Tukey's test. Asterisks indicate significant difference (** $p < 0.01$, * $p < 0.05$).

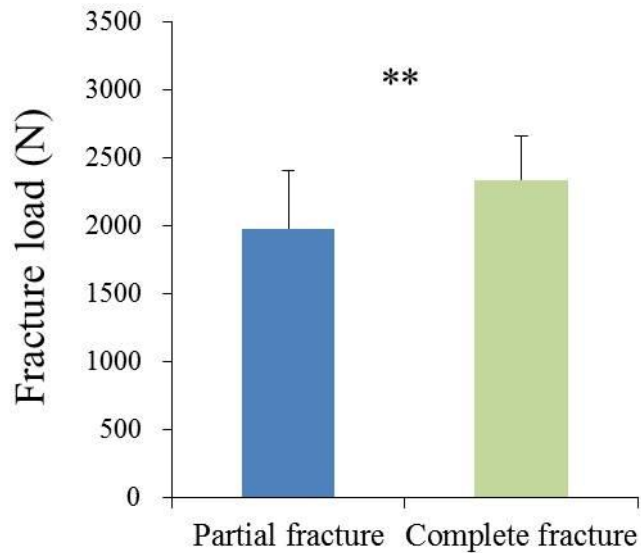


Figure 48. Comparison of fracture loads between different failure modes. Asterisks indicate significant difference (** $p < 0.01$).

11.0 Acknowledgments

I would like to thank to Prof. Dr. Jürgen Geis-Gerstorfer, Director of the Section Medical Materials Science and Technology, Dental Faculty, Eberhard Karls University Tübingen, Germany for supporting and advising my disseration.

I'm very grateful to Prof. Dr. Heiner Weber, Medical director, Department of Prosthodontics, Center for Dentistry and Oral Medicine, Eberhard Karls University Tübingen, to your offer.

My special appreciation to Mr. Sebastian Spintzk, ZTM Ekkehard Kröwerath, Ms. Christine Schille, Mr. Ernst Schweizer (University Hospital Tübingen) and ZTM Kazunari Ohata (DENTAL LABOR GROSS GmbH, Tokyo, Japan) for their help, support, and advice.

I would also like to thank Mr. Fumio Sugata and Mr. Tomohiro Udaka from Panasonic Healthcare for advising the framework design and providing the zirconia framework.

Finally, I would like to thank my family for their support throughout my study, especially, my father (Prof. Dr. Tomoji Sawada) and my wife.

12.0 Curriculum Vitae

Name: Tomofumi Sawada

Date of birth: 18.02.1979

Birthplace: Kanagawa, Japan

Nationality: Japanese

EDUCATION

Year	Degree	Major Area	Affiliation
1997–2003	D.D.S	Dentistry	School of Dentistry, Kanagawa Dental College
2005–2009	Ph.D.	Prosthodontics	Graduate School, Kanagawa Dental College

Professional History

Year	Official Position	Affiliation
2003–2004	Resident	Department of Prosthodontics, Showa University, School of Dentistry
2004–2005	Clinical Fellow	Division of Removal Prosthetics, Department of Oral and Maxillofacial Rehabilitation, Kanagawa Dental College, Kanagawa
2009–2012	Assistant Professor	Division of Fixed Prosthodontics, Department of

Oral and Maxillofacial Rehabilitation, Kanagawa
Dental College

2012–2013 Lecturer Division of Fixed Prosthodontics, Department of
Oral and Maxillofacial Rehabilitation, Kanagawa
Dental College

2013– Guest Scientist Department of Prosthodontics and Section Medical
Materials Science & Technology Center of
Dentistry, Oral Medicine, and Maxillofacial Surgery,
University of Tübingen

Science Activity

27-28.08.15 Poster presentation at the 23rd European Dental Materials Conference in
Nürnberg.

Sawada T, Spintzyk S, Udaka T, Schille C, Schweizer E, Sugata F,
Geis-Gerstorfer J. 2015. Influence of fracture strength on different
zirconia framework designs. Eur J Prosthodont Rest Dent. Special Issue:
p33.

05.05.16 Part of the manuscript has been published in Materials.

Sawada T, Spintzyk S, Schille C, Schweizer E, Scheideler L,
Geis-Gerstorfer J. Influence of different framework designs on the
fracture properties of ceria-stabilized tetragonal zirconia/alumina based
all-ceramic crowns. Materials. 9:339.2016.